ZETA EXPANSION FOR LONG-RANGE INTERACTIONS UNDER PERIODIC BOUNDARY CONDITIONS WITH APPLICATIONS TO MICROMAGNETICS

ANDREAS A. BUCHHEIT, JONATHAN K. BUSSE, TORSTEN KESSLER, AND FILIPP N. RYBAKOV

ABSTRACT. We address the efficient computation of power-law-based interaction potentials of homogeneous d-dimensional bodies with an infinite n-dimensional array of copies, including their higher-order derivatives. This problem forms a serious challenge in micromagnetics with periodic boundary conditions and related fields. Nowadays, it is common practice to truncate the associated infinite lattice sum to a finite number of images, introducing uncontrolled errors. We show that, for general interacting geometries, the exact infinite sum for both dipolar interactions and generalized Riesz power-law potentials can be obtained by complementing a small direct sum by a correction term that involves efficiently computable derivatives of generalized zeta functions. We show that the resulting representation converges exponentially in the derivative order, reaching machine precision at a computational cost no greater than that of truncated summation schemes. In order to compute the generalized zeta functions efficiently, we provide a superexponentially convergent algorithm for their evaluation, as well as for all required special functions, such as incomplete Bessel functions. Magnetic fields can thus be evaluated to machine precision in arbitrary cuboidal domains periodically extended along one or two dimensions. We benchmark our method against known formulas for magnetic interactions and against direct summation for Riesz potentials with large exponents, consistently achieving full precision. In addition, we identify new corrections to the asymptotic limit of the demagnetization field and tabulate high-precision benchmark values that can be used as a reliable reference for micromagnetic solvers. The techniques developed are broadly applicable, with direct impact in other areas such as molecular dynamics.

1. INTRODUCTION AND PROBLEM DESCRIPTION

Microscopic textures of magnetization in magnetic materials are extremely diverse, interesting for applications, and challenging to observe and explain. Numerous studies with a century-long history are devoted to the theory of micromagnetic states [47, 64, 46, 4, 12, 23, 52, 43, 25]. The "micromagnetics" formulated back in 1959 [14, 3, 13] is a powerful theoretical approach to understand these phenomena. Approaches to solving micromagnetic problems can be divided into two large classes: with the explicit involvement of magnetic field potential (either scalar or vector one) or without it [5, 26]. Naturally, both approaches have their advantages and disadvantages.

The well-known advantages of potential-based approaches include those provided by finite element methods. Namely, the ability to accurately simulate samples of
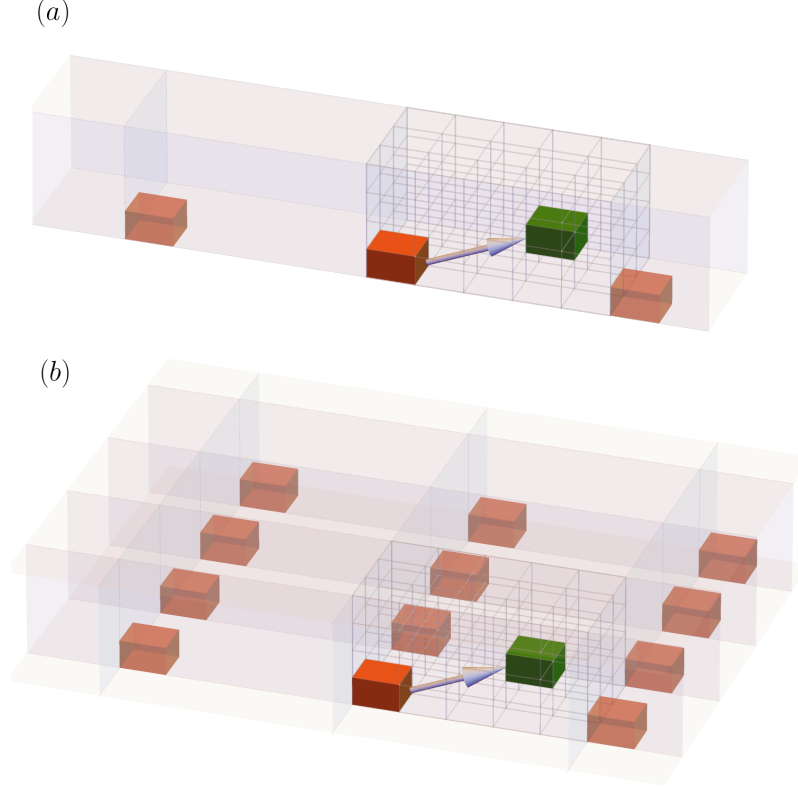
(a)

(b)

FIGURE 1. Sketch illustrating a 3D system of of $N_x \times N_y \times N_z = 5 \times 3 \times 4$ interacting cuboids repeated infinitely in x direction (a), and both in x and y direction (b). The green cuboid is influenced by the red cuboid indicated by the arrow, as well as by the total influence of all opaque red cuboids

complex shapes by representing them as composed of simplices such as tetrahedrons. At the same time, it is challenging to accurately account for fields outside the sample – semi-infinite regions where the decay has an algebraic nature. There is a large literature devoted to the relevant methods; for finite elements in micromagnetics, see Refs. [61, 42, 1, 35], and for exterior issues, i.g. Neumann-to-Dirichlet map, see Refs. [44, 53, 28]. However, there is an important and interesting feature here. In those dimensions where periodic boundary conditions (PBC) are assumed, the non-trivial component of the potential field is naturally a periodic function, and, accordingly, the problem of semi-infinities disappears along the corresponding dimensions.

On the other hand, potential-free approaches are well applicable for rectangular geometries. One strong advantage is the translation invariance when discretized by identical cuboids (rectangular prisms). The calculation of the interaction of "everyone with everyone" is accelerated by applying the fast Fourier transform (FFT) and the convolution theorem for zero-padded arrays [70, 56, 43]. Convolution

kernels can be precomputed once for a given geometry and used at each iteration as constant arrays. However, in contrast to potential-based methods, the challenge here is precisely the case of PBC, see Fig. 1. This is because the convolution kernel requires calculating sums of infinite and slowly converging series for each of the dimensions with PBC, see [48]. It is important to emphasize that in modern studies, these sums are approximated by a naive cutoff technique. For example, in popular software packages such as MuMax3 [67], the corresponding parameter, SetPBC(int, int, int), is the number of "repeats", and due to the related time consumption, these integers rarely exceed the value of 10, see e.g. the Supplemental Material in [62] and Refs. [57, 8, 66, 45]. Some other relevant software packages are as follows: OOMMF [27], BORIS [49], magnum.np [15], Ubermag [36]. The above-mentioned sums cannot be reliably approximated by classic techniques such as Ewald summation [34], although in some special cases, such as when the cuboids are cubes, there is numerical evidence of significant improvement in accuracy [48]. In general, the problem exists because the interaction potentials are functions with rather complex profiles such as compositions of power, trigonometric and hyperbolic functions, which are further complicated by dependencies on the aspect ratios of the cuboid (see Refs. [58, 43] and A). As a result, truncating the series and/or replacing functions with simpler ones when calculating dipole-dipole interactions leads to an inconsistency of the boundary conditions in the sense that the periodicity of local interactions is exact, but that of non-local interactions is inaccurate. This causes discrepancies that can no longer be reduced by mesh refinement.

The present work solves this problem. Some of the authors have recently generalized the classic Euler–Maclaurin summation formula to include power-law long-range interactions on higher-dimensional lattices [18, 16, 19], leading to the singular Euler-Maclaurin (SEM) expansion. This method allows to exactly describing discrete lattices in terms of their continuous analogs with an efficiently computable correction term [19]. In a recent major advancement, we have extended this method to lattice subsets with boundaries [16]. These methods are based on efficiently computable generalized zeta functions [17] and allow for the computation of non-trivial high-dimensional lattice sums and their meromorphic continuations to full precision. In this work, we further generalize this framework to the use case appearing in micromagnetics. We show how to compute interaction energies in domains $\Omega \subset \mathbb{R}^d$, typically three-dimensional cuboids, with infinite arrays of periodic images, arising from general Riesz-type long-range interactions of the form $|\boldsymbol{r}|^{-\nu}$, including their meromorphic continuation in ν efficiently to full precision. Importantly, our framework supports the evaluation of interaction energy derivatives of arbitrary order. By choosing derivatives up to order 2 and $\nu = 1$, we recover all quantities required for the simulation of micromagnetic systems in d dimensions, periodically repeated along an n-dimensional subarray with $n < d$. Note that for micromagnetic problems, the natural dimension of space is $d = 3$, and lattices are typically one-dimensional ($n = 1$) or two-dimensional ($n = 2$), which corresponds to the geometry of wires, Fig. 1(a), or films, Fig. 1(b), respectively. The method, however, extends to general interactions and geometries.

We begin our exposition by introducing the generalized interaction potential of a body Ω with an array of copies, each centered at a point in a set $L \subseteq \mathbb{R}^d$.

Definition 1.1 (Generalized potential with periodic boundary conditions)**.** Let Ω be a compact domain in $\mathbb{R}^d$. We define the potential function of a source object

Ω located at position $\boldsymbol{r} \in \mathbb{R}^d$, interacting with an n-dimensional arbitrary Bravais lattice L in d-dimensional space of identical objects. For an interaction exponent $\nu > n$, and a multi-index of derivative orders $\boldsymbol{m} \in \mathbb{N}^d$, the potential reads

$$(1) \qquad U^{(\boldsymbol{m})}(\boldsymbol{r}) = \sum_{\boldsymbol{z} \in L} \int_{\Omega + \boldsymbol{z}} \nabla_{\boldsymbol{r}}^{\boldsymbol{m}} \int_{\Omega + \boldsymbol{r}} |\boldsymbol{r}' - \boldsymbol{r}''|^{-\nu} \, \mathrm{d}\boldsymbol{r}' \, \mathrm{d}\boldsymbol{r}''.$$

The potential can be meromorphically continued to $\nu \in \mathbb{C}$.

The above potential function allows to evaluate all potentials and magnetic fields appearing in micromagnetics. While highly efficient methods exist for evaluating the double integral for single summands, see A, the evaluation of the infinite and slowly decaying lattice sum has posed severe computational problems so far, as we described above. Fast methods for kernel evaluation like the Fast Multipole Method [40, 22] and related methods like Adaptive Cross Approximation [6, 7] or polynomial interpolation [9, Chapter 4] speed up the nested integrals over the interaction potential as they separate the integral into two independent ones. But they do not accelerate the convergence of the infinite sum as the leading terms of the corresponding expansions only decay algebraically and hence do not improve the slow convergence of the infinite sum. In contrast, here we leverage efficiently computable generalizations of the Riemann zeta function to compute the infinite lattice sum at a negligible additional cost in runtime compared to standard methods that truncate the real space sum. This permits the precise and efficient study of periodic magnetic textures with long-range interactions with vast application potential.

This work is structured as follows. In Section 2, we present our efficiently computable representation of the generalized micromagnetics potential. In Section 3, we subsequently compare our method against direct summation for large exponents and against known results, obtaining full precision across the complete parameter range. We further obtaining new asymptotic corrections to known formulas for the demagnetization field and provide high-precision reference values for future implementations in micromagnetics packages. In Section 4, we discuss how to efficiently evaluate all special functions, which are required for our algorithm. In particular, we discuss how to evaluate the arising incomplete Bessel functions to full precision. We draw our conclusions and briefly describe how the results of this work can be applied to other problems in condensed matter physics and other disciplines in Section 5.

2. Main result

In this work, we solve the problem of efficiently computing the infinite sums that arise in micromagnetic simulations to full precision. Our approach divides the sum into two parts, a small direct sum, already implemented in standard packages such as MuMax3, and a correction term that eliminates the truncation error. We then show that this correction term can be expressed in terms of derivatives of a generalized zeta function. By presenting an efficient algorithm for computing these derivatives to full precision, we enable the evaluation of the infinite lattice sum at essentially the same numerical cost as the truncated sum.

We will need Fourier transforms in the following, for which we choose the following convention.

Definition 2.1 (Fourier transformation). For an integrable function $f : \mathbb{R}^d \to \mathbb{C}$ the Fourier transformation $\mathcal{F} : f \mapsto \hat{f}$ is given by

$$\hat{f}(\boldsymbol{\xi}) = \int_{\mathbb{R}^d} f(\boldsymbol{x}) e^{-2\pi i \boldsymbol{x} \cdot \boldsymbol{\xi}} \, d\boldsymbol{x}, \quad \boldsymbol{\xi} \in \mathbb{R}^d.$$

We subsequently define the zeta function for a point set $L \subseteq \mathbb{R}^d$, shifted by a vector $\boldsymbol{r} \in \mathbb{R}^d$.

Definition 2.2 (Set zeta function). Let $L \subseteq \mathbb{R}^d$ be a uniformly discrete set, $\boldsymbol{r} \in \mathbb{R}^d$, and $\nu \in \mathbb{C}$ with $\mathrm{Re}(\nu) > d$. We then define the zeta function of the set $L \backslash \{\boldsymbol{r}\}$ as the meromorphic continuation of

$$Z_{L,\nu}(\boldsymbol{r}) = \sideset{}{'}\sum_{\boldsymbol{z} \in L} \frac{1}{|\boldsymbol{z} - \boldsymbol{r}|^\nu},$$

to $\nu \in \mathbb{C}$, where the primed sum excludes the summand where $\boldsymbol{z} = \boldsymbol{r}$.

Note that in contrast to [16], the argument of the zeta function here refers to the shift in position. The resulting zeta function is related to the Epstein zeta function originally introduced by Paul Epstein in 1903 in [29, 30]. For some some lattice $\Lambda = A\mathbb{Z}^d$, $A \in \mathbb{R}^{d \times d}$ regular, a shiftvector $\boldsymbol{r} \in \mathbb{R}^d$, and a wavevector $\boldsymbol{k} \in \mathbb{R}^d$, the Epstein zeta function is defined as the lattice sum

$$Z_{\Lambda,\nu} \begin{vmatrix} \boldsymbol{r} \\ \boldsymbol{k} \end{vmatrix} = \sideset{}{'}\sum_{\boldsymbol{z} \in \Lambda} \frac{e^{-2\pi i \boldsymbol{k} \cdot \boldsymbol{z}}}{|\boldsymbol{z} - \boldsymbol{r}|^\nu}, \qquad \mathrm{Re}(\nu) > d,$$

meromorphically continued to $\nu \in \mathbb{C}$. The Epstein zeta function is a generalization of the Riemann zeta function to oscillatory lattice sums in multiple dimensions and is of particular interest in the physics of long-range interacting lattice systems [21]. The set zeta function was recently introduced by some of the authors in [16] as a generalization to geometries without translational invariance.

The following theorem is our first main result. It provides a way to correct the error introduced by truncating the lattice sum through efficiently computable derivatives of zeta functions, yielding an exact expression for the full sum. We refer to this method as *zeta expansion*. To present the result in a compact form, we adopt standard multi-index notation, i.e., $\boldsymbol{\alpha}! = \alpha_1! \alpha_2! \dots \alpha_d!$. The proof relies on the fact that the set zeta function is holomorphic in $\boldsymbol{r}$ on a subset of $\mathbb{C}^d$, see Corollary 2.6, and can be expanded into a Taylor series that converges uniformly on every ball that does not intersect L. This Corollary follows directly from Theorem 2.5 that also yields a computationally efficient representation of the infinite sum.

Theorem 2.3 (Zeta expansion for micromagnetics). *Consider* $L = A\mathbb{Z}^n \times \{0\}^{d-n}$ *with* $A \in \mathbb{R}^{n \times n}$ *regular and* $n \in \mathbb{N}_+$ *with* $n \leq d$, *a multi-index of derivative orders* $\boldsymbol{m} \in \mathbb{N}^d$, *and a compact domain* $\Omega \subset \mathbb{R}^d$. *For* $\boldsymbol{r} \in \mathbb{R}^d$, *choose a symmetric near-field lattice* $L_{\mathrm{near}} \subset L$ *such that* $-L_{\mathrm{near}} = L_{\mathrm{near}}$ *and a far-field lattice* $L_{\mathrm{far}} = L \setminus L_{\mathrm{near}}$ *such that* $\mathrm{dist}_\infty(\boldsymbol{r}, L_{\mathrm{far}} + 2\Omega) > 0$ *with* dist_∞ *the distance in the infinity norm.*

The potential admits the near/far-field decomposition,

$$U^{(\boldsymbol{m})}(\boldsymbol{r}) = \sum_{\boldsymbol{z} \in L_{\mathrm{near}}} S^{(\boldsymbol{m})}(\boldsymbol{r} + \boldsymbol{z}) + \mathcal{Z}_{L_{\mathrm{far}}}^{(\boldsymbol{m})}(\boldsymbol{r})$$

with a truncated sum over $S^{(\boldsymbol{m})}(\boldsymbol{r})$,

$$S^{(\boldsymbol{m})}(\boldsymbol{r}) = \int_\Omega \nabla_{\boldsymbol{r}}^{\boldsymbol{m}} \int_{\Omega + \boldsymbol{r}} |\boldsymbol{r}' - \boldsymbol{r}''|^{-\nu} \, d\boldsymbol{r}' \, d\boldsymbol{r}''.$$

The correction term $\mathcal{Z}_{L_{\text{far}}}^{(\boldsymbol{m})}(\boldsymbol{r})$ can be expressed in terms of a zeta function acted on by a shape-dependent differential operator $\mathcal{D}_\Omega$,

$$\mathcal{Z}_{L_{\text{far}}}^{(\boldsymbol{m})}(\boldsymbol{r}) = \mathcal{D}_\Omega Z_{L_{\text{far}},\nu}^{(\boldsymbol{m})}(\boldsymbol{r}).$$

For a general compact domain Ω, the operator admits the convergent Taylor representation

$$\mathcal{D}_\Omega = \sum_{\boldsymbol{\alpha} \geq \boldsymbol{0}} \frac{1}{\boldsymbol{\alpha}!} \, \mathcal{I}_{\boldsymbol{\alpha}}(\Omega) \, \nabla^{\boldsymbol{\alpha}}, \qquad \mathcal{I}_{\boldsymbol{\alpha}}(\Omega) = \iint_{\Omega \times \Omega} (\boldsymbol{r} - \boldsymbol{r}')^{\boldsymbol{\alpha}} \, \mathrm{d}\boldsymbol{r} \, \mathrm{d}\boldsymbol{r}',$$

where, if Ω is centrally symmetric, $\Omega = -\Omega$, only multi-indices $\boldsymbol{\alpha}$ with all components even contribute, since otherwise $\mathcal{I}_{\boldsymbol{\alpha}}(\Omega) = 0$.

For the axis-aligned cuboid $\Omega = \prod_{i=1}^{d} (-c_i/2, c_i/2)$, $c_j > 0$, the operator $\mathcal{D}_\Omega$ takes the explicit form

$$\mathcal{D}_\Omega = \sum_{\boldsymbol{\alpha} \geq \boldsymbol{0}} \frac{2^d}{(2(\boldsymbol{\alpha}+\boldsymbol{1}))!} \, \boldsymbol{c}^{2(\boldsymbol{\alpha}+\boldsymbol{1})} \nabla^{2\boldsymbol{\alpha}}, \qquad \boldsymbol{c} = (c_1, \ldots, c_d)^T.$$

with $\boldsymbol{1} = (1, \ldots, 1)^T$.

Proof. We begin by removing the sum over L_{near}. In the remaining sum over L_{far}, notice that the derivative with respect to $\boldsymbol{r}'$ can be interchanged with the derivative with respect to $\boldsymbol{r}$ due to linearity. By Fubini's theorem, we can exchange the order of integration and differentiation, leading to

$$\mathcal{Z}_{L_{\text{far}}}^{(\boldsymbol{m})}(\boldsymbol{r}) = \iint_{\Omega \times \Omega} Z_{L_{\text{far}},\nu}^{(\boldsymbol{m})}(\boldsymbol{r} - \boldsymbol{r}') \, \mathrm{d}\boldsymbol{r} \, \mathrm{d}\boldsymbol{r}'.$$

Now, by holomorphy of the set zeta function from Corollary 2.6, and by the restriction on the distance of $\boldsymbol{r}$ to L_{far}, the integrand and all its derivatives can be expanded in uniformly convergent Taylor series within this domain, yielding

$$\mathcal{Z}_{L_{\text{far}}}^{(\boldsymbol{m})}(\boldsymbol{r}) = \iint_{\Omega \times \Omega} \sum_{\boldsymbol{\alpha} \geq \boldsymbol{0}} \frac{(\boldsymbol{r} - \boldsymbol{r}')^{\boldsymbol{\alpha}}}{\boldsymbol{\alpha}!} Z_{L_{\text{far}},\nu}^{(\boldsymbol{m}+\boldsymbol{\alpha})}(\boldsymbol{0}) \, \mathrm{d}\boldsymbol{r} \, \mathrm{d}\boldsymbol{r}' = \sum_{\boldsymbol{\alpha} \geq \boldsymbol{0}} \frac{\mathcal{I}_{\boldsymbol{\alpha}}(\Omega)}{\boldsymbol{\alpha}!} Z_{L_{\text{far}},\nu}^{(\boldsymbol{m}+\boldsymbol{\alpha})}(\boldsymbol{0}),$$

where the order of integration and summation was exchanged due to Fubini. For the case of the cuboid, the moment integral factorizes component-wise and we have

$$\int_{-c_i/2}^{c_i/2} \int_{-c_i/2}^{c_i/2} (r_i - r_i')^{\alpha_i} \, \mathrm{d}r_i \, \mathrm{d}r_j = \frac{2c_i^{\alpha_i+2}}{(\alpha_i + 1)(\alpha_i + 2)}, \quad \text{all } \alpha_i \text{ even,}$$

and zero otherwise. Recombining $\mathcal{I}_{\boldsymbol{\alpha}}(\Omega)$ then yields the specific form of the operator for the cuboid. $\qquad \square$

By enlarging the real space sum, we increase the radius of analyticity of the zeta function $Z_{L_{\text{far}},\nu}(\boldsymbol{r})$ around $\boldsymbol{0}$. As a result, the larger the real space sum, and the smaller the size of Ω, the fewer derivatives need to be included to reach full precision. These derivatives of the zeta function can then be written in terms of a truncated sum plus two superexponentially convergent sums, all of which can be efficiently evaluated.

The error when truncating the number of derivatives falls off exponentially in the number of derivaties and algebraically in the components of $\boldsymbol{c}$. The precise error scaling is described in the following corollary.

Corollary 2.4 (Error scaling)**.** *Assume the conditions of Theorem 2.3 hold. Fix $\eta > 1$, such that*

$$\mathrm{dist}_\infty(\mathbf{0}, L_{\mathrm{far}} + 2\Omega) > \eta\, d\, \mathrm{diam}(\Omega),$$

with $\mathrm{diam}(\Omega) = \sup_{\mathbf{r},\mathbf{r}'\in\Omega} \|\mathbf{r} - \mathbf{r}'\|_\infty$ *the diameter of Ω. For any $\mathbf{r} \in \mathbb{R}^d$, such that*

$$\|\mathbf{r}\|_\infty < \eta\, d\, \mathrm{diam}(\Omega),$$

and $\ell \in \mathbb{N}$, the remainder when truncating to derivatives of order $|\boldsymbol{\alpha}| \leq \ell$,

$$R_\ell = \sum_{|\boldsymbol{\alpha}|>\ell} \frac{1}{\boldsymbol{\alpha}!}\, \mathcal{I}_{\boldsymbol{\alpha}}(\Omega)\, \nabla^{\boldsymbol{\alpha}} Z^{(\boldsymbol{m})}_{L_{\mathrm{far}},\nu}(\mathbf{r}),$$

can be uniformly bounded in $\mathbf{r}$ by

$$|R_\ell| \leq M\big(\mathrm{Vol}(\Omega)\big)^2 \frac{\eta^{-\ell}}{(\eta-1)}$$

where $M = \sup\{Z^{(\boldsymbol{m})}_{L_{\mathrm{far}},\nu}(\mathbf{z}) : \mathbf{z} \in \mathbb{C}^d,\ \|\mathbf{z}\|_\infty < \eta\, d\, \mathrm{diam}(\Omega)\}$.

Proof. By Corollary 2.6, $Z^{(\boldsymbol{m})}_{L_{\mathrm{far}}}(\cdot)$ is holomorphic on the polydisc

$$\mathbb{D} = \{\mathbf{z} \in \mathbb{C}^d : \|\mathbf{z}\|_\infty < \rho\}$$

with radius $\rho = \eta\, d\, \mathrm{diam}(\Omega)$. From Cauchy's estimate follows,

$$\sup_{\mathbf{z}\in\mathbb{D}} |\nabla^{\boldsymbol{\alpha}} Z^{(\boldsymbol{m})}_{L_{\mathrm{far}},\nu}(\mathbf{z})| \leq M \frac{\boldsymbol{\alpha}!}{\rho^{|\boldsymbol{\alpha}|}}.$$

Using further that

$$I_{\boldsymbol{\alpha}}(\Omega) = \iint_{\Omega\times\Omega} (\mathbf{r} - \mathbf{r}')^{\boldsymbol{\alpha}}\, \mathrm{d}\mathbf{r}\, \mathrm{d}\mathbf{r}' \leq (\mathrm{diam}(\Omega))^{|\boldsymbol{\alpha}|} (\mathrm{Vol}(\Omega))^2$$

we can bound the remainder by

$$|R_\ell| \leq M(\mathrm{Vol}(\Omega))^2 \sum_{|\boldsymbol{\alpha}|>\ell} (\eta d)^{-|\boldsymbol{\alpha}|}.$$

After setting $\mathbf{q} = \mathbf{1}/(\eta d)$ and thus $(\eta d)^{-|\boldsymbol{\alpha}|} = \mathbf{q}^{\boldsymbol{\alpha}}$, the multinomial theorem yields for $k \in \mathbb{N}$,

$$\sum_{|\boldsymbol{\alpha}|=k} \mathbf{q}^{\boldsymbol{\alpha}} \leq \sum_{|\boldsymbol{\alpha}|=k} \frac{k!}{\boldsymbol{\alpha}!} \mathbf{q}^{\boldsymbol{\alpha}} = (q_1 + \cdots + q_d)^k = (d/(\eta d))^k = \eta^{-k}.$$

After evaluating the geometric series,

$$\sum_{k=\ell+1}^{\infty} \eta^{-k} = \frac{\eta^{-\ell}}{(\eta-1)},$$

we obtain the asserted bound. $\qquad\square$

As our second main result, we present a representation of the set zeta function and its derivatives in terms of superexponentially decaying sums. The resulting representation serves as the basis for its efficient computation and can be used to derive the properties of the generalized zeta function. We name this representation Crandall representation due to the close connection to the exponentially convergent representation of the Epstein zeta function derived by Crandall in [24]. The underlying method can be considered as a generalization of Ewald summation [34].

Theorem 2.5 (Crandall representation of set zeta functions). *Let $L = A\mathbb{Z}^n \times \{0\}^{d-n}$, $n \in \mathbb{N}_+$ with $n \leq d$, and $\boldsymbol{\alpha} \in \mathbb{N}^d$. For $\boldsymbol{r} \in \mathbb{R}^d$, choose a finite near-field lattice $L_{\mathrm{near}} \subset L$ and set $L_{\mathrm{far}} = L \setminus L_{\mathrm{near}}$. Adopt the notation $\boldsymbol{r}^{\|} = (r_1, \ldots, r_n)^T$ and $\boldsymbol{r}^{\perp} = (r_{n+1}, \ldots, r_d)^T$ and likewise for $\boldsymbol{\alpha}$. For $\mathrm{Re}(\nu) > n$, derivatives of the zeta function of the far-field lattice then admit the representation*

$$Z_{L_{\mathrm{far}},\nu}^{(\boldsymbol{\alpha})}(\boldsymbol{r}) = \frac{(\pi/\lambda^2)^{\nu/2}}{\Gamma(\nu/2)} \Bigg[\sum_{\boldsymbol{z} \in L_{\mathrm{far}}} \lambda^{-|\boldsymbol{\alpha}|} G_{\nu}^{(\boldsymbol{\alpha})}\Big(\frac{\boldsymbol{z} - \boldsymbol{r}}{\lambda}\Big) - \sum_{\boldsymbol{z} \in L_{\mathrm{near}}} \lambda^{-|\boldsymbol{\alpha}|} g_{\nu}^{(\boldsymbol{\alpha})}\Big(\frac{\boldsymbol{z} - \boldsymbol{r}}{\lambda}\Big)$$

$$+ \frac{\lambda^n}{V_{\Lambda}} \sum_{\boldsymbol{k} \in \Lambda^*} (-2\pi i \boldsymbol{k})^{\boldsymbol{\alpha}^{\|}} e^{-2\pi i \boldsymbol{k} \cdot \boldsymbol{r}^{\|}} \lambda^{-|\boldsymbol{\alpha}^{\perp}|} G_{n-\nu}^{(\boldsymbol{\alpha}^{\perp})}\Big(\lambda \boldsymbol{k}, \frac{\boldsymbol{r}^{\perp}}{\lambda}\Big) \Bigg].$$

where $\Lambda^* = A^{-T}\mathbb{Z}^n$ and where $\lambda > 0$ denotes the Riemann splitting parameter and where the derivative always acts with respect to $\boldsymbol{r}$ (or $\boldsymbol{r}^{\perp}$). Furthermore, we define the upper Crandall function G_{ν} and the lower Crandall function g_{ν} as

$$G_{\nu}(\boldsymbol{z}) = \frac{\Gamma(\nu/2, \pi \boldsymbol{z}^2)}{(\pi \boldsymbol{z}^2)^{\nu/2}}, \qquad g_{\nu}(\boldsymbol{z}) = \frac{\gamma(\nu/2, \pi \boldsymbol{z}^2)}{(\pi \boldsymbol{z}^2)^{\nu/2}},$$

with $\Gamma(a, z)$ the upper and $\gamma(a, z)$ the lower incomplete Gamma function. Here $g_{\nu}(\boldsymbol{z})$ is continuously extended to $\boldsymbol{z} = \boldsymbol{0}$ and we define $G_{\nu}(\boldsymbol{0}) = -\nu/2$. Finally, $G_{\nu}(\boldsymbol{k}, \boldsymbol{r})$ is an incomplete Bessel function,

$$G_{\nu}(\boldsymbol{k}, \boldsymbol{r}) = 2 \int_0^1 t^{-\nu} e^{-\pi \boldsymbol{k}^2/t^2} e^{-\pi \boldsymbol{r}^2 t^2} \frac{\mathrm{d}t}{t}.$$

The representation forms the meromorphic continuation to $\nu \in \mathbb{C}$.

Proof. We follow the proof of [17, Th. 2.11] and begin by deriving the Crandall representation for $\boldsymbol{\alpha} = \boldsymbol{0}$. Let $\nu > d$, so the defining lattice sum of the set zeta function converges absolutely by [17, Lemma A.1.]. Note that the lattice sum is no longer primed, as $\boldsymbol{r} \notin L_{\mathrm{far}}$. By the fundamental relation for the Crandall functions [17, Lemma 2.9 (2)]

$$(\boldsymbol{z}^2)^{-\nu/2} \frac{\Gamma(\nu/2)}{(\pi/\lambda^2)^{\nu/2}} = G_{\nu}(\boldsymbol{z}/\lambda) + g_{\nu}(\boldsymbol{z}/\lambda)$$

we may separate the set zeta function into the upper and lower Crandall functions with a Riemann splitting parameter $\lambda > 0$. Further separating the sum involving the lower Crandall functions into a sum over the complete set L minus a near-field sum yields

$$Z_{L_{\mathrm{far}},\nu}(\boldsymbol{r}) \frac{\Gamma(\nu/2)}{(\pi/\lambda^2)^{\nu/2}} = \sum_{\boldsymbol{z} \in L_{\mathrm{far}}} G_{\nu}\Big(\frac{\boldsymbol{z} - \boldsymbol{r}}{\lambda}\Big) - \sum_{\boldsymbol{z} \in L_{\mathrm{near}}} g_{\nu}\Big(\frac{\boldsymbol{z} - \boldsymbol{r}}{\lambda}\Big) + \sum_{\boldsymbol{z} \in L} g_{\nu}\Big(\frac{\boldsymbol{z} - \boldsymbol{r}}{\lambda}\Big).$$

For the sum over the whole set $L = \Lambda \times \{0\}^{d-n}$, $\Lambda = A\mathbb{Z}^n$, we obtain

$$\sum_{\boldsymbol{z} \in L} g_{\nu}\Big(\frac{\boldsymbol{z} - \boldsymbol{r}}{\lambda}\Big) = 2 \int_0^1 t^{-\nu} \Big(\sum_{\boldsymbol{z}^{\|} \in \Lambda} e^{-\pi(\boldsymbol{z}^{\|} - \boldsymbol{r}^{\|})^2 t^2/\lambda^2}\Big) e^{-\pi(\boldsymbol{r}^{\perp})^2 t^2/\lambda^2} \frac{\mathrm{d}t}{t}.$$

by the integral representation for the lower Crandall function in the proof of [16, Lem. 2.10], where we exchanged the sum and the integral by dominant convergence for $\mathrm{Re}(\nu) > n$. After applying Poisson summation [17, Lem. 2.6] to the sum over Λ with the Fourier transform

$$\mathcal{F}\big(e^{-\pi(\cdot - \boldsymbol{r}^{\|})^2 t^2/\lambda^2}\big)(\boldsymbol{k}) = \lambda^n t^{-n} e^{-2\pi i \boldsymbol{k} \cdot \boldsymbol{r}^{\|}} e^{-\pi \boldsymbol{k}^2 \lambda^2/t^2},$$

we obtain

$$\sum_{\boldsymbol{z} \in L} g_\nu\left(\frac{\boldsymbol{z} - \boldsymbol{r}}{\lambda}\right) = \frac{\lambda^n}{V_\Lambda} \sum_{\boldsymbol{k} \in \Lambda^*} e^{-2\pi i \boldsymbol{k} \cdot \boldsymbol{r}^\|} G_{n-\nu}\left(\lambda \boldsymbol{k}, \frac{\boldsymbol{r}^\perp}{\lambda}\right).$$

Applying the derivative to the reassembled formula yields the statement. $\qquad\square$

The holomorphic extension of the set zeta function, and thus its radius of analyticity, readily follows from the Crandall representation.

Corollary 2.6. *Let the conditions of Theorem 2.5 hold and define the set* $D_{L_{\text{far}}} \subseteq \mathbb{C}^d$ *as an intersection of d-dimensional complex cones centered at the point set* $L_{\text{far}} \subseteq \mathbb{R}^d$,

$$D_{L_{\text{far}}} = \{\boldsymbol{u} \in \mathbb{C}^d : |\text{Re}(\boldsymbol{u}) - \boldsymbol{z}| > |\text{Im}(\boldsymbol{u})| \ \forall \boldsymbol{z} \in L_{\text{far}}\}.$$

Then $Z_{L_{\text{far}},\nu}$ *extends to a holomorphic function on* $D_{L_{\text{far}}}$.

Proof. For $\boldsymbol{r}^\perp = \boldsymbol{0}$, the function corresponds to an Epstein zeta function minus a finite sum over L_{near}. Here, the holomorphy of $G_\nu(\cdot)$ on

$$D = \{\boldsymbol{u} \in \mathbb{C}^d : |\text{Re}(\boldsymbol{u})| > |\text{Im}(\boldsymbol{u})|\}$$

and for $g_\nu(\cdot)$ on $\mathbb{C}^d$ has been shown in [20, Lemma 2.9] and the resulting holomorphy of the Epstein zeta function has been proven in [20, Theorem 2.13]. This result then directly applies to the set zeta function.

For $\boldsymbol{r}^\perp \neq \boldsymbol{0}$, notice from the integral representation of the incomplete Crandall function that for $\boldsymbol{k} \neq \boldsymbol{0}$, $G_{n-\nu}(\boldsymbol{k}, \boldsymbol{r}^\perp)$ is entire in $\boldsymbol{r}^\perp$ with the bound.

$$|G_{n-\nu}(\boldsymbol{k}, \boldsymbol{r}^\perp)| < |G_{n-\nu}(\boldsymbol{k})|.$$

For $\boldsymbol{k} = \boldsymbol{0}$, the function reduces to a lower Crandall function, which is entire too. Thus, the set zeta function is holomorphic on $D_{L_{\text{near}}}$ as the compactly uniformly limit of holomorphic functions. $\qquad\square$

As the Crandall functions (and their derivatives) exhibit the asymptotic scaling

$$|G_\nu(\boldsymbol{k}, \boldsymbol{r})| \leq |G_\nu(\boldsymbol{r})| \sim \frac{e^{-\pi \boldsymbol{r}^2}}{\pi \boldsymbol{r}^2},$$

see [16, 17], both sums fall off at a superexponential rate, building the foundation for an efficient computation of the zeta function.

Note that all derivatives of the Crandall functions can be expressed analytically in terms of other Crandall functions with shifted exponents, as discussed in Sec. 4. The complete algorithm for computing the set zeta function for arbitrary parameter choices is also presented there. Combining these results, Theorem 2.3 provides the exact correction of lattice sums due to truncation in terms of derivatives of generalized zeta functions, while Theorem 2.5 establishes a superexponentially convergent representation of the required zeta functions and their derivatives. Together with the error scaling in Corollary 2.4, these results enable the efficient computation of the potential function and all its derivatives needed in micromagnetics.

3. Numerical results

3.1. **Comparison against direct summation.** Establishing reliable analytic benchmarks for non-trivial infinite lattice sums is a challenging task, as exact formulas are scarce, see, e.g., [10] and references therein. In the following, we use the fact that our method admits an arbitrary exponent ν, and compare our method for
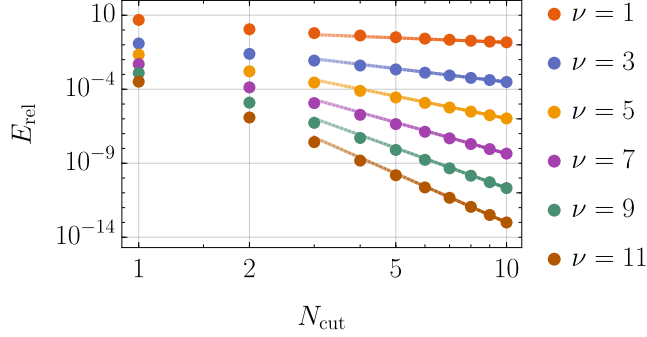
FIGURE 2. Relative error between the three-dimensional potential $U^{(0,0,2)}(\boldsymbol{r})$ centered at $\boldsymbol{r} = (1,1,1)/2$ for the lattice at $\mathbb{Z}^2 \times \{0\}$ as obtained by the zeta representation in Theorem 2.3 in comparison with direct summation over the truncated grid $\{-N_{\text{cut}}, \ldots, N_{\text{cut}}\}^2 \times \{0\}$ as dots a function of the the truncation length integers $1 \leq N_{\text{cut}} \leq 10$. The error scaling $C_\nu N_{\text{cut}}^{-\nu}$ for some fitted parameter C_ν is shown as lines of the in the same color as the corresponding the error dots.

sufficiently large ν with direct summation, which still yields high-precision reference values within reasonable times.

To this end, we study the interaction potential $U^{(\boldsymbol{m})}(\boldsymbol{r})$ for the cuboid domain $\Omega = \prod_{i=1}^3 [-c_i/2, c_i/2]$ centered at $\boldsymbol{r}$ for some $\boldsymbol{c} \in \mathbb{R}_+^3$ with an infinite 2D array of copies centered at $L = \mathbb{Z}^2 \times \{0\}$. Let E_{rel} denote the relative error of our algorithm in comparison with high-precision values obtained by direct summation over the truncated lattice $\{-N_{\text{cut}}, \ldots, N_{\text{cut}}\}^2 \times \{0\}$ for some $N_{\text{cut}} \in \mathbb{N}_+$. Furthermore, we choose $L_{\text{near}} = \{-1, 0, 1\}^2 \times \{0\}$ in the near/far-field decomposition in Theorem 2.3 for the zeta treatment of the potential. For benchmarking our implementation of the potential, we take $\nu \geq 10$ and $N_{\text{cut}} = 14$. We compare the potential obtained by adding the zeta-correction with up to fourth-order derivatives to the 9 summands in the grid $L_{\text{near}} = \{-1, 0, 1\}^2 \times \{0\}$ with the potential obtained by summing over the truncated lattice consisting of 841 summands. In Table 1 we show the error for fixed second-order derivatives

$$\boldsymbol{m} \in \{(1,1,0), (1,0,1), (0,0,2)\}$$

and geometries

$$\boldsymbol{c} \in \{(1,1,1)/50, (1,1,1)/100, (1,2,3)/100\}.$$

over a grid of values $\boldsymbol{r} = (1/4, 1/4, r)$, $r \in \{1/10, 2/10, \ldots, 5/10\}$ and $\nu \in [10, 15]$ in increments of $1/10$. where the direct sum converges at least proportional to N_{cut}^{-10}. We observe, that our algorithm reaches full precision over the whole parameter range. As the error of our method does not exhibit a relevant scaling with ν, see Corollary 2.4, a corresponding precision is to be expected for the whole ν range, which is confirmed by another analytic benchmark in the next section.

Assuming on this basis that the value of the zeta method is numerically exact, we now study the convergence of the direct sum against this reference for $\boldsymbol{m} = (0,0,2)^T$

derivative vector $\boldsymbol{m}$	cuboid geometry $\boldsymbol{c}$	$\max_{\boldsymbol{r},\nu} E_{\mathrm{rel}}$
$(1,1,0)$	$(1,1,1)/50$	$2.16 \cdot 10^{-16}$
	$(1,1,1)/100$	$2.12 \cdot 10^{-16}$
	$(1,2,3)/100$	$2.20 \cdot 10^{-16}$
$(1,0,1)$	$(1,1,1)/50$	$2.18 \cdot 10^{-16}$
	$(1,1,1)/100$	$2.11 \cdot 10^{-16}$
	$(1,2,3)/100$	$2.16 \cdot 10^{-16}$
$(0,0,2)$	$(1,1,1)/50$	$3.87 \cdot 10^{-16}$
	$(1,1,1)/100$	$2.14 \cdot 10^{-16}$
	$(1,2,3)/100$	$2.19 \cdot 10^{-16}$

TABLE 1. Relative error of the potential $U^{(\boldsymbol{m})}(\boldsymbol{r})$ of a cuboid cuboid $\Omega = \prod_{i=1}^{3}[-c_i/2, c_i/2]$ centered at $\boldsymbol{r}$ and its images centered at lattice points $L = \mathbb{Z}^2 \times \{0\}$ for different second-order derivatives $\boldsymbol{m}$ and geometries $\boldsymbol{c}$. The value computed by our method with $N_{\mathrm{cut}} = 1$ including up to fourth-order derivatives in the zeta correction term, is compared to direct summation with $N_{\mathrm{cut}} = 14$ at sufficiently large values of ν, where a reliable reference can still be obtained within reasonable times. Each error is the maximum error obtained over a grid of values $\boldsymbol{r} = (1/4, 1/4, r)$ for $1/10 \leq r \leq 1/2$ and $10 \leq \nu \leq 14$ in increments of $\Delta r = \Delta \nu = 1/10$.

and small values of ν as a function of the truncation N_{cut} in Figure 2. We find that the relative error scales as $N_{\mathrm{cut}}^{-\nu}$, leading to slow convergence for small values of ν. For the case of micromagnetics, $\nu = 1$, and a typically used value of $N_{\mathrm{cut}} = 10$, the relative error compared to the zeta method still exceeds $15\,\%$.

3.2. **Corrections to asymptotic behavior of the demagnetization field.** As a second benchmark, we compare our numerical method against analytic expressions for the leading asymptotic behavior of the demagnetization factor. To this end, we consider a three-dimensional cuboid $\Omega = [-c/2, c/2]^3$, centered at $\boldsymbol{r} = \boldsymbol{0}$, and its infinite repetitions along the lattice $\Lambda = \mathbb{Z}^2$, with the cuboid being magnetized along the z-axis. Dividing the elementary lattice cell into N cuboids per dimension yields $c = 1/N$, see Figure 3.

The demagnetization factor D_z then reads,

$$D_z = 1 + \frac{1}{4\pi} \frac{1}{c^3} \left(U^{(2,0,0)}(\boldsymbol{0}) + U^{(0,2,0)}(\boldsymbol{0}) \right),$$

and thus reflects both the influence of the cuboid's own field (see A) and the impact of an infinite number of neighbors. We provide the values of D_z beyond machine precision in Table 2 . One useful observation is that for $N = 1$, the system develops into a continuous planar layer (of thickness c), and therefore the demagnetization factor is trivial:
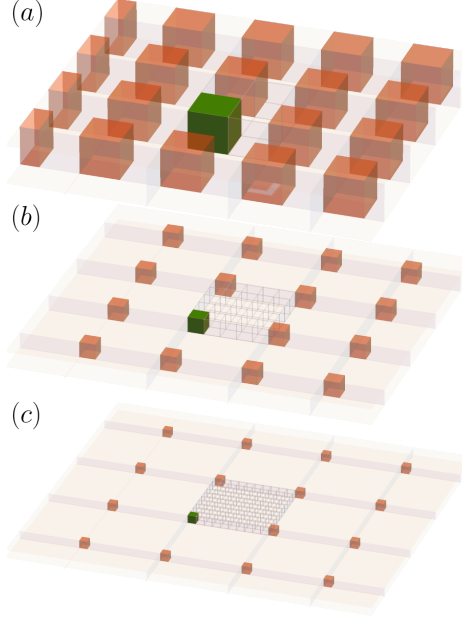
$$D_z = 1 \quad (N = 1).$$

FIGURE 3. Cuboid $\Omega = [1/(2N), 1/(2N)]^3$ and its infinite repetitions $z + \Omega$ along the two-dimensional lattice embedded in three dimensions $L = \mathbb{Z}^2 \times \{0\}$ for $N = 2$ (a), $N = 5$ (b) and $N = 10$ (c).

On the other hand, for $N \to \infty$, the cuboid is small compared to the lattice spacing, such that it interacts with its repetitions as a point dipole. The magnetic field contribution from the copies is expressed through a lattice sum, where the leading asymptotic corrections due to finite size of the cuboid can be analytically determined [11], yielding

$$D_z^{\mathrm{asym}} = \frac{1}{3} + \frac{Z_{\mathbb{Z}^2,3}(\mathbf{0})}{4\pi} \frac{1}{N^3},$$

with the particular value of the Epstein zeta function [71, Table 1, Sum $S(0,2)$]

$$Z_{\mathbb{Z}^2,3}(\mathbf{0}) = 4\beta(3/2)\zeta(3/2),$$

and where β denotes the Dirichlet beta function.

In Fig. 4, we display the absolute difference between the demagnetization factor, obtained from the zeta expansion, and the known asymptotic formula as a function of N. We reproduce the known asymptotic behavior, providing another validation for our approach. In addition, we obtain the next order asymptotic correction,

$$D_z = D_z^{\mathrm{asym}} - \alpha \frac{1}{N^7}, \quad N \to \infty,$$

where $\alpha \approx 0.1441459732$ has been obtained from a fit. This correction results from the $|\boldsymbol{\alpha}| = 1$ terms in the zeta expansion in Theorem 2.3.

To serve as a reliable benchmark for future implementations of our algorithm in micromagnetics software packages, we provide multi-precision values of the demagnetization factor for various values of N in Table 2.

N	D_z
2	0.4222 0496 3454 0001 7334 0215 3861 9290
5	0.3390 8248 7690 9804 5966 0589 1398 9491
10	0.3340 5219 1717 7249 3459 0417 7785 8568
50	0.3333 3908 4315 3283 8944 2139 2339 3160
100	0.3333 3405 2206 1043 3571 9460 7573 5189

TABLE 2. High-precision evaluation of the demagnetization factor D_z for different values of $N \in \{2, 5, 10, 50, 100\}$ for 32 digits of precision. For $N = 2$ we chose $L_{\text{near}} = \{-26, \ldots, -26\}^2 \times \{0\}$ and derivatives up to the 10'th order in the zeta correction term and for $N \geq 5$ we chose $L_{\text{near}} = \{-22, \ldots, -22\}^2 \times \{0\}$ and derivatives up to the 8th-order in the zeta correction term. The zeta correction term was calculated over the grid $\{-6, \ldots, 6\}^3$.
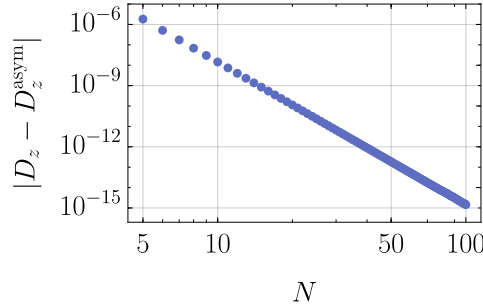

FIGURE 4. Difference between demagnetization factor D_z for 3D cuboids $\Omega = [-1/(2N), 1/(2N)]^3$ interacting with a lattice $\Lambda = \mathbb{Z}^2$, computed from our method, and the known asymptotic formula. The asymptotic behavior is correctly reproduced, as well as the corner cases ($D_z = 1$ for $N = 1$ and $D_z \to 1/3$ for $N \to \infty$). The next order correction from the known asymptotics as $N \to \infty$ scales as N^{-7} (obtained by a fit).

4. COMPUTATION OF GENERALIZED ZETA FUNCTIONS

In this section, we present the ingredients required for the efficient evaluation of the set zeta function. Theorem 2.3 provides the foundation for this evaluation. Following the algorithm for computing the Epstein zeta function in [17], we set $\lambda = 1$ and rescale the lattice so that $V_\Lambda = 1$. Since both the real- and reciprocal-space sums decay at a superexponential rate, they may be truncated to only a small number of lattice points near the origin. A tight cutoff will be derived in forthcoming work.

The Crandall functions appearing in the representation can be evaluated to full precision using the algorithm in [17]. Their derivatives, which are also required, can be expressed in terms of Crandall functions, as described in Sec. 4.1. In

the reciprocal-space sum, incomplete Bessel functions arise. Their evaluation is addressed in detail in Sec. 4.2.

4.1. **Analytic representation of derivatives.** All derivatives of the Crandall functions can be computed analytically in terms of other Crandall functions.

Lemma 4.1 (Derivatives of Crandall functions). *Let $\nu \in \mathbb{C}$, $\boldsymbol{\alpha} \in \mathbb{N}^d$, and $\boldsymbol{r}, \boldsymbol{k} \in \mathbb{R}^d \setminus \{\boldsymbol{0}\}$. Then*

$$G_\nu^{(\boldsymbol{\alpha})}(\boldsymbol{r}) = \sum_{|\boldsymbol{\beta}| \leq |\boldsymbol{\alpha}|/2} p_{\boldsymbol{\alpha},\boldsymbol{\beta}}(\boldsymbol{r}) G_{\nu+2|\boldsymbol{\alpha}|-2|\boldsymbol{\beta}|}(\boldsymbol{r}),$$

$$g_\nu^{(\boldsymbol{\alpha})}(\boldsymbol{r}) = \sum_{|\boldsymbol{\beta}| \leq |\boldsymbol{\alpha}|/2} p_{\boldsymbol{\alpha},\boldsymbol{\beta}}(\boldsymbol{r}) g_{\nu+2|\boldsymbol{\alpha}|-2|\boldsymbol{\beta}|}(\boldsymbol{r}),$$

$$G_\nu^{(\boldsymbol{\alpha})}(\boldsymbol{k},\boldsymbol{r}) = \sum_{|\boldsymbol{\beta}| \leq |\boldsymbol{\alpha}|/2} p_{\boldsymbol{\alpha},\boldsymbol{\beta}}(\boldsymbol{r}) G_{\nu-2|\boldsymbol{\alpha}|+2|\boldsymbol{\beta}|}(\boldsymbol{k},\boldsymbol{r}),$$

where the derivative always acts on $\boldsymbol{r}$ and where $p_{\boldsymbol{\alpha},\boldsymbol{\beta}}$ is the following monomial,

$$p_{\boldsymbol{\alpha},\boldsymbol{\beta}}(\boldsymbol{r}) = (-\pi)^{|\boldsymbol{\alpha}|-|\boldsymbol{\beta}|} \binom{\boldsymbol{\alpha}}{\boldsymbol{\beta}} \frac{(\boldsymbol{\alpha}-\boldsymbol{\beta})!}{(\boldsymbol{\alpha}-2\boldsymbol{\beta})!} (2\boldsymbol{r})^{\boldsymbol{\alpha}-2\boldsymbol{\beta}}.$$

Furthermore, the derivatives of the Crandall functions extend continuously to $\boldsymbol{r} = \boldsymbol{0}$ with

$$G_\nu^{(\boldsymbol{\alpha})}(\boldsymbol{0}) = -2\chi(\boldsymbol{\alpha}) \frac{p_{\boldsymbol{\alpha},\boldsymbol{\alpha}/2}(\boldsymbol{0})}{\nu+|\boldsymbol{\alpha}|}, \qquad\qquad \mathrm{Re}(\nu) + |\boldsymbol{\alpha}| < 0,$$

$$g_\nu^{(\boldsymbol{\alpha})}(\boldsymbol{0}) = 2\chi(\boldsymbol{\alpha}) \frac{p_{\boldsymbol{\alpha},\boldsymbol{\alpha}/2}(\boldsymbol{0})}{\nu+|\boldsymbol{\alpha}|}, \qquad\qquad \mathrm{Re}(\nu) + |\boldsymbol{\alpha}| > 0,$$

where the right-hand sides form the meromorphic continuation to $\nu \in \mathbb{C} \setminus \{-|\boldsymbol{\alpha}|\}$. Here, $\chi(\boldsymbol{\alpha}) = 1$ if every entry of $\boldsymbol{\alpha}$ is even and $\chi(\boldsymbol{\alpha}) = 0$ otherwise. Finally, in the case of $\mathrm{Re}(\nu) - |\boldsymbol{\alpha}| < 0$, the derivative of the incomplete bessel function extends continuously to $\boldsymbol{r} = \boldsymbol{0}$ and $\boldsymbol{k} = \boldsymbol{0}$ with

$$G_\nu^{(\boldsymbol{\alpha})}(\boldsymbol{0},\boldsymbol{0}) = -2\chi(\boldsymbol{\alpha}) \frac{p_{\boldsymbol{\alpha},\boldsymbol{\alpha}/2}(\boldsymbol{0})}{\nu-|\boldsymbol{\alpha}|}$$

where the right-hand side forms the meromorphic continuation to $\nu \in \mathbb{C} \setminus \{|\boldsymbol{\alpha}|\}$.

Proof. The formulas for the derivatives of the upper and lower Crandall functions follow directly from their integral representation. For the incomplete Bessel function, inserting the integral representation yields

$$G_\nu^{(\boldsymbol{\alpha})}(\boldsymbol{k},\boldsymbol{r}) = \sum_{|\boldsymbol{\beta}| \leq |\boldsymbol{\alpha}|/2} p_{\boldsymbol{\alpha},\boldsymbol{\beta}}(\boldsymbol{r}) 2 \int_0^1 t^{-\nu+2|\boldsymbol{\alpha}|-2|\boldsymbol{\beta}|} e^{-\pi k^2/t^2} e^{-\pi r^2 t^2} \frac{\mathrm{d}t}{t}$$

and in the case of $\mathrm{Re}(\nu) - |\boldsymbol{\alpha}| < 0$, $\chi(\boldsymbol{a}) = 1$ and $\boldsymbol{\beta} = \boldsymbol{\alpha}/2$ we obtain

$$\lim_{h \to 0_+} G_{\nu-|\boldsymbol{\alpha}|}(h\boldsymbol{k}, h\boldsymbol{r}) = 2 \int_0^1 t^{-(\nu-|\boldsymbol{\alpha}|)-1} \mathrm{d}t = -\frac{2}{\nu-|\boldsymbol{\alpha}|}.$$

By dominant convergence and by the identity theorem, $-2\chi(\boldsymbol{\alpha}) p_{\boldsymbol{\alpha},\boldsymbol{\alpha}/2}(\boldsymbol{0})/(\nu-|\boldsymbol{\alpha}|)$ provides the unique holomorphic continuation of $G_\nu^{(\boldsymbol{\alpha})}(\boldsymbol{0},\boldsymbol{0})$ to $\nu \in \mathbb{C} \setminus \{|\boldsymbol{\alpha}|\}$. $\qquad\square$

Remark 4.2. The multinomial coefficient $\binom{\boldsymbol{\alpha}}{\boldsymbol{\beta}}$ found in the polynomial $p_{\boldsymbol{\alpha},\boldsymbol{\beta}}(\cdot)$ in Lemma 4.1 can be efficiently evaluated as the product of d one-dimensional binomial coefficients, see [39] and the fraction

$$\frac{(\boldsymbol{\alpha} - \boldsymbol{\beta})!}{(\boldsymbol{\alpha} - 2\boldsymbol{\beta})!}$$

can be be obtained by multiplication of at most $\lfloor \boldsymbol{\alpha}/2 \rfloor$ numbers.

4.2. Computation of the incomplete Bessel function.
In this section, we discuss how the incomplete Bessel function in Theorem 2.5 can be evaluated to full precision. The algorithm is mainly based on the series expansion in [41] and the recursive algorithm in [63]. In the following, we focus on $\nu \in \mathbb{R}$.

An algorithm for the computation of the incomplete Bessel function is presented in Algorithm 1. The different evaluations regions of the Algorithm 1 are shown in Figure 5. In what follows, we discuss the procedures employed in Algorithm 1 and show the the error is flat over the whole parameter range.

For at least one vanishing vector argument, the incomplete Bessel function reduces to the upper and lower Crandall functions, readily available in EpsteinLib.

Lemma 4.3. *Let $\nu \in \mathbb{R} \setminus \{0\}$, then*

$$G_\nu(\mathbf{0}, \mathbf{0}) = -\frac{2}{\nu}.$$

Let $\nu \in \mathbb{R}$ and $\boldsymbol{k} \in \mathbb{R}^d$, then

$$G_\nu(\boldsymbol{k}, \mathbf{0}) = G_\nu(\boldsymbol{k}).$$

Let $\boldsymbol{r} \in \mathbb{R}^d$ where $\boldsymbol{r} \neq \mathbf{0}$ if $\nu \in 2\mathbb{N}$, then

$$G_\nu(\mathbf{0}, \boldsymbol{r}) = g_{-\nu}(\boldsymbol{r}).$$

Proof. The integral representation of $G_\nu(\boldsymbol{k}, \mathbf{0})$ reduces to the integral representation of $G_\nu(\boldsymbol{k})$ in [17, Lemma B.1.], yielding in particular $G_\nu(\mathbf{0}, \mathbf{0}) = G_\nu(\mathbf{0}) = -2/\nu$. Furthermore, $G_\nu(\mathbf{0}, \boldsymbol{r})$ reduces to the second integral representation of $g_{-\nu}(\boldsymbol{r}/\lambda)$ for $\lambda = 1$, as shown in the proof [17, Lemma 2.10]. □

We may always swap non-zero vector arguments at the cost of computing a modified Bessel function of the second kind, as the following lemma shows. This allows us to restrict our computation to incomplete Bessel functions where $\boldsymbol{k}^2 + C > \boldsymbol{r}^2$ for some $C > 0$, where the algorithm achieves superior numerical stability.

Lemma 4.4 (Incomplete Bessel reflection formula). *Let $\nu \in \mathbb{R}$, and let $\boldsymbol{k}, \boldsymbol{r} \in \mathbb{R}^d \setminus \{\mathbf{0}\}$. Then*

$$G_\nu(\boldsymbol{k}, \boldsymbol{r}) = 2(\boldsymbol{r}^2/\boldsymbol{k}^2)^{\nu/4} K_{\nu/2}(2\pi\sqrt{\boldsymbol{k}^2\boldsymbol{r}^2}) - G_{-\nu}(\boldsymbol{r}, \boldsymbol{k})$$

where $K_\nu(2z)$, $s \in \mathbb{R}$, $z > 0$ is the modified Bessel function of the the second kind

$$K_\nu(2z) = \frac{z^\nu}{2} \int_0^\infty t^{-\nu} e^{-t - z^2/t} \frac{\mathrm{d}t}{t}.$$

Proof. Substitute $s = 1/t$ in the integral representation of the incomplete Bessel function in Theorem 2.5 to obtain

$$G_\nu(\boldsymbol{k}, \boldsymbol{r}) = \int_0^\infty 2t^\nu e^{-\pi\boldsymbol{k}^2 t^2} e^{-\pi\boldsymbol{r}^2/t^2} \frac{\mathrm{d}t}{t} - G_{-\nu}(\boldsymbol{r}, \boldsymbol{k}),$$

Algorithm 1: Computation of the incomplete Bessel function.

Input: $\nu \in \mathbb{R}$, $\boldsymbol{k}, \boldsymbol{r} \in \mathbb{R}^d$

$x = \pi \boldsymbol{k}^2; \quad y = \pi \boldsymbol{r}^2; \quad s = -\nu/2$

```
/* Vanishing arguments                                        */
```
if $x + y = 0$ **then**
    return $1/s$

```
/* Vanishing first arguments                                  */
```
if $x = 0$ **then**
    return $g_{-\nu}(\boldsymbol{r})$

```
/* Vanishing second arguments                                 */
```
if $y = 0$ **then**
    return $G_\nu(\boldsymbol{k})$

```
/* Vanishing upper bound                                      */
```
if $2\sqrt{\pi}\, x^{-(\nu+1)/4} y^{(\nu-1)/4} e^{(\nu^2/16 - 2xy)/\sqrt{xy}} < 10^{-16}$ **then**
    return 0

```
/* Reflect parameters for upper half of the plane             */
```
if $x + 1/5 < y$ **then**
    swap = True; $\quad (s, x, y) \leftarrow (-s, y, x)$
else
    swap = False

```
/* Choose series expansion/recursive algorithm                */
```
if $x + y < 3/2$ **then**
    result $= G_{-2s}(\boldsymbol{k})$
    for $j = 1, \ldots, 20$ **do**
        result $\mathrel{+}= G_{-2(s+j)}(\boldsymbol{k})(-y)^j/j!$
else
    $n_1 = 0; \quad n_2 = 0; \quad n_3 = 1$
    $d_1 = 0; \quad d_2 = e^{x+y}; \quad d_3 = (x - y + s + 1)d_2$
    for $j = 2, \ldots, 100$ **do**
        $N = ((x - y + s + 1 + 2(j-1))n_3 + (2y - s - (j-1))n_2 - yn_1)/j$
        $D = ((x - y + s + 1 + 2(j-1))d_3 + ((2y - s - (j-1))d_2 - yd_1)/j$
        $n_1 = n_2; \quad n_2 = n_3; \quad n_3 = N$
        $d_1 = d_2; \quad d_2 = d_3; \quad d_3 = D$
    result $= N/D$

```
/* Reflect result for upper half of the plane                 */
```
if swap **then**
    result $\leftarrow 2(x/y)^{s/2} K_s(2\sqrt{xy}) - $ result

return result

---

where we have extended the integration domain to $(0, \infty)$, by adding and subtracting the integral from 0 to 1. After setting $u = \pi \boldsymbol{k}^2 t^2$, the integral above takes the form

$$\left(\frac{1}{\pi \boldsymbol{k}^2}\right)^{\nu/2} \int_0^\infty u^{\nu/2} e^{-u - \pi^2 \boldsymbol{k}^2 \boldsymbol{r}^2/u} \, \frac{\mathrm{d}u}{u} = 2(\boldsymbol{r}^2/\boldsymbol{k}^2)^{\nu/4} K_{-\nu/2}(2\pi\sqrt{\boldsymbol{k}^2 \boldsymbol{r}^2})$$
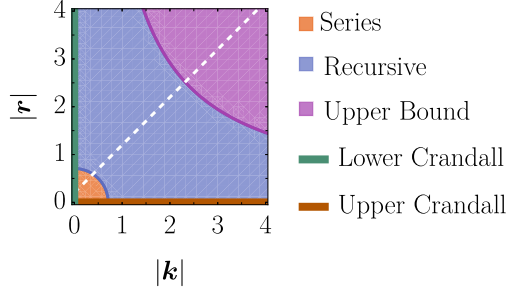
FIGURE 5. Regions of Algorithm 1. The white line indicates the split, where above the dashed white line we employ the reciprocal values. The purple region where the upper bound of the incomplete Bessel function is smaller than 10^{-16} is shown for $\nu = 0$.

and the statement follows from the symmetry $K_s(z) = K_{-s}(z)$ [31, Sec. 7.2.2, Eq. (14)]. $\qquad\square$

For small vector arguments, we may now use the series expansion in the second variable [41, Eq. (16)]. For intermediate vector arguments, we employ the recursive algorithm due to [63]. For large vector arguments, we may assume the incomplete Bessel function to be zero, if the following upper bound is smaller than 10^{-16}.

Lemma 4.5. *Let $\nu \in \mathbb{R}$, and let $\boldsymbol{k}, \boldsymbol{r} \in \mathbb{R}^d \setminus \{\boldsymbol{0}\}$. Then*

$$G_\nu(\boldsymbol{k}, \boldsymbol{r}) \le 2(\boldsymbol{k}^2)^{-(\nu+1)/4}(\boldsymbol{r}^2)^{(\nu-1)/4} \exp\left(\frac{\nu^2}{16\pi\sqrt{\boldsymbol{k}^2\boldsymbol{r}^2}} - 2\pi\sqrt{\boldsymbol{k}^2\boldsymbol{r}^2} \right).$$

Proof. Following the proof of Lemma 4.4 we have

$$G_\nu(\boldsymbol{k}, \boldsymbol{r}) \le 2(\boldsymbol{r}^2/\boldsymbol{k}^2)^{\nu/4} K_s(2z)$$

for $s = \nu/2$, $z = \pi\sqrt{\boldsymbol{k}^2\boldsymbol{r}^2}$. An upper bound to the modified Bessel function is readily obtained from the integral representation [31, Sec. 17.12, Eq. (21)],

$$K_s(2z) = \int_0^\infty \cosh(st) e^{-2z\cosh t} \, \mathrm{d}t.$$

As $1 + s^2/2 \le \cosh s \le e^{|s|}$, we find that

$$K_s(2z) \le e^{-2z} \int_0^\infty e^{-z(t^2 - |s|t/z)} \, \mathrm{d}t.$$

After completing the squares $t^2 - |s|t/z = (t - |s|/(2z))^2 - s^2/(4z^2)$ and extending the integration range to $(-\infty, \infty)$ we obtain

$$K_s(2z) \le e^{s^2/(4z)-2z} \int_{-\infty}^\infty e^{-z(t-|s|/(2z))^2} \, \mathrm{d}t$$

where the Gaussian integral evaluates to $\sqrt{\pi/z}$. $\qquad\square$

We now assess the precision and runtime of incomplete Bessel function evaluations by Algorithm 1. Let E denote the minimum of the absolute and relative error

$$E = \min\{E_{\mathrm{abs}}, E_{\mathrm{rel}}\}$$

ν	E_{med}	E_{max}	$t_{\mathrm{med}}\,[s]$	$t_{\mathrm{max}}\,[s]$
-4	$1.18 \cdot 10^{-17}$	$4.91 \cdot 10^{-15}$	$1 \cdot 10^{-6}$	$1 \cdot 10^{-5}$
-2	$1.24 \cdot 10^{-17}$	$3.14 \cdot 10^{-15}$	$1 \cdot 10^{-6}$	$5 \cdot 10^{-6}$
0	$1.26 \cdot 10^{-17}$	$4.88 \cdot 10^{-15}$	$1 \cdot 10^{-6}$	$8 \cdot 10^{-6}$
2	$1.34 \cdot 10^{-17}$	$4.55 \cdot 10^{-15}$	$1 \cdot 10^{-6}$	$5 \cdot 10^{-6}$

TABLE 3. Minimum of absolute and relative error of $G_\nu(\boldsymbol{r}, \boldsymbol{k})$ obtained by Algorithm 1 for $\nu = \{-4, -2, 0, 2\}$. Every value corresponds to the a grid of $1/10 \le |\boldsymbol{r}|, |\boldsymbol{k}| \le 4$ with with $1/10$. Reference values obtained by high precision integral evaluations.

of our algorithm in comparison with high-precision values obtained by the integral representation. In Table 3 we show the median and maximal error E_{med} and E_{max} as well as the median and maximum evaluation times t_{med} and t_{max} over the parameter grid $0 \le |\boldsymbol{k}|, |\boldsymbol{r}| \le 4$ of width $1/20$ for some fixed $\nu \in \{-4, -2, 0, 2\}$. Note, that we skip the singular cases for $\boldsymbol{k} = \boldsymbol{r} = \boldsymbol{0}$, $\nu = 0$ and $\boldsymbol{k} = \boldsymbol{0}$, $\boldsymbol{r} \neq \boldsymbol{0}$, $\nu \in 2\mathbb{N}$. We achieve machine precision $E < 5 \cdot 10^{-15}$ over the whole parameter range for evaluation times of $t \le 10^{-5}$ seconds. The values were obtained on an Intel Core i7-1260P (12th Gen) 16-core processor.

5. Outlook and discussion

In this work, we have presented an efficient and precise method for evaluating infinite lattice sums appearing in micromagnetics with periodic boundary conditions. At the moment of writing of this work, a common practice was to truncate the arising sums, leading to an uncontrolled source of error. We show that the error due to truncation can be removed by an additional efficiently computable correction term that follows from a generalization of the Riemann zeta function to sums over n-dimensional lattices in d-dimensional space. We present an efficient way to compute the arising zeta functions, including their derivatives, and implement the resulting algorithm in a high-performance C framework. Benchmarks of algorithm against known formulas and direct summation for large interaction exponents show that full precision is reached, while the numerical effort for the correction term is much smaller than the effort for typical truncated sums. This makes it possible to reach machine precision for the infinite sum at effectively the same runtime than truncated sums in current software packages.

The implications of this work are twofold. First, quantitative errors due to truncation in micromagnetic systems with periodic boundary conditions can be removed at a negligible numerical cost, yielding reliable results. Second, since our method is general and applies to arbitrary interaction exponents, source and target geometries, and lattices, it can be applied to other problems. In order to be specific, we briefly describe a few examples below.

Ferroelectrics. Microscopic textures in ferroelectrics are essentially the spatial distribution of the polarization vector, $\mathbf{P}(\mathbf{r})$, within the sample. These textures are very diverse and are the subject of intensive research [54, 50]. If there are no free electric charges in the sample, i.e. the charge distribution is described solely by polarization, then the application of our method is straightforward due to

electromagnetic duality. That is, instead of the magnetization vector $\mathbf{M}$ (see A) we assume the polarization vector $\mathbf{P}$, plus the corresponding replacement for vector potentials, $\mathbf{A} \mapsto \mathbf{F}$ (electric vector potential), and fields, $\mathbf{B} \mapsto \mathbf{E}$ (electric field).

In cases where Ω is a point source, there is no need for integration and derivatives for the potential of Eq. (1) as the problem is reduced to the discrete one, while the method we propose here is anyway, a generalization of the previous results [18, 16, 19] where $n = d$ to cases $n < d$. The following examples may apply to these new cases.

Atomistic spin dynamics. Classical spin models [32, 65] are related to micromagnetics within certain limits, while in the general case, these are different problems. Spin-spin interactions can exhibit slowly decaying interactions in addition to the dipole–dipole interaction, such as the Ruderman-Kittel-Kasuya-Yosida (RKKY) interaction. Accordingly, our new method can be applied to model magnetic multilayers such as van-der-Waals magnets and beyond.

Qualitatively new behavior can be studied in systems where different phases exhibit minute energy differences, i.e. in frustrated systems. Similar phenomena have recently been observed in a new Shastry-Sutherland Ising compound and have been theoretically explained using computational techniques that are precursors to this work [69].

Molecular dynamics. Periodic boundary conditions are a natural approach in molecular dynamics for interpreting unbounded dimensions. The case $n < d$ is of particular interest, since it is well-known that confinement affects phase transitions, e.g. in the ultra-thin water films [38]. In turn, the functions of intermolecular potentials can have rather complex and slowly decaying profiles of the Lennard-Jones type and others [59]. Accordingly, our new method can significantly improve numerical techniques for studying such systems.

As a final remark, we emphasize that the high-precision values presented in Table 2 can be regarded as fundamental constants of micromagnetics and, in particular, serve as reliable references for benchmarking numerical methods.

Data Availability

The authors declare that all data supporting the findings of this work are available within this article. The open-source library EpsteinLib is publicly available, see [17]. The implementation of the incomplete Bessel function is available on GitHub (github.com/JoKaBus/incomplete-bessel) and includes a notebook `examples/mathematica/MicromagneticsReplicated.wls` that reproduces the numerical results presented in this article.

Appendix A. Homogeneous cuboid in micromagnetics

In this section, we present explicit expressions for the magnetic fields generated by a uniformly magnetized cuboid (rectangular prism). We also provide formulas for the demagnetization factors and the interaction energy of two cuboids. To the best of our knowledge, previous approaches to this problem in the literature were based on rather cumbersome analytical calculations [58, 60, 55, 43, 2]. In contrast, here we propose a compact approach based on the theory of the potential [51] and Hertz potentials in electromagnetism [33].
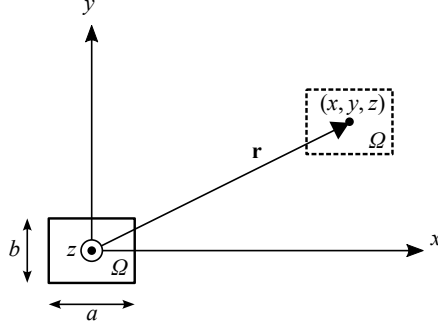
FIGURE 6. Cuboid Ω centered in the Cartesian coordinate system (x, y, z).

We consider a cuboid-shaped source (domain Ω) of size $a \times b \times c$ placed in the center of the Cartesian coordinate system, see Fig. 6. We call the cuboid a source, meaning that each of its points is considered by us as a source of Newtonian potential, $\sim \frac{1}{|\mathbf{r}|}$. The total potential of a cuboid is calculated by integration and can be represented [68] in the following canonical form:

$$(A1) \qquad \Phi(x, y, z) = \sum_{i,j,k=\pm 1} i\,j\,k\,F_1\left(x + i\tfrac{a}{2}, y + j\tfrac{b}{2}, z + k\tfrac{c}{2}\right),$$

with the auxiliary function

$$F_1(u, v, w) = -\frac{u^2}{2}\arctan\left(\frac{v\,w}{u\,R}\right) - \frac{v^2}{2}\arctan\left(\frac{w\,u}{v\,R}\right) - \frac{w^2}{2}\arctan\left(\frac{u\,v}{w\,R}\right) +$$
$$+ v\,w\,\mathrm{artanh}\left(\frac{u}{R}\right) + w\,u\,\mathrm{artanh}\left(\frac{v}{R}\right) + u\,v\,\mathrm{artanh}\left(\frac{w}{R}\right),$$

and $R \equiv \sqrt{u^2 + v^2 + w^2}$. Using Φ, we can explicitly write the expression for the Hertz magnetic vector [33] of uniformly magnetized cuboid:

$$(A2) \qquad \mathbf{Z}(\mathbf{r}) = \frac{\mu_0}{4\pi}\,\mathbf{M}\,\Phi(\mathbf{r}),$$

where $\mu_0 = 4\pi \times 10^{-7}$ N/A^2, and $\mathbf{M} \equiv (M_x, M_y, M_z)$ is the magnetization vector (in A/m). Magnetic vector potential and magnetic field are derived quantities:

$$(A3) \qquad \mathbf{A}(\mathbf{r}) \equiv \nabla \times \mathbf{Z}(\mathbf{r}),$$

$$(A4) \qquad \mathbf{B}(\mathbf{r}) \equiv \nabla \times \mathbf{A}(\mathbf{r}) = \frac{\mu_0}{4\pi}\,\nabla \times \nabla \times (\mathbf{M}\,\Phi(\mathbf{r})).$$

We are further interested in the integral result of the action of the magnetic field described by Eq. (A4) on some displaced domain of shape Ω, see Fig. 6:

$$(A5) \qquad \mathbf{B}_{\mathrm{avg}}(\mathbf{r}) = \frac{\int_{\Omega+\mathbf{r}} \mathbf{B}(\mathbf{r}')\,d\mathbf{r}'}{\int_{\Omega+\mathbf{r}} d\mathbf{r}'} = \frac{1}{a\,b\,c} \int_{\Omega+\mathbf{r}} \mathbf{B}(\mathbf{r}')\,d\mathbf{r}'.$$

The components of this vector are linear combinations of the potentials from Eq. (1) for $\nu = 1$, $n = 0$ and $d = 3$ (trivial case for a single cuboid in three-dimensional space), namely

$$\mathbf{B}_{\mathrm{avg}}(\mathbf{r}) = \frac{\mu_0}{4\pi\,a\,b\,c} \times$$

$$\mathbf{M} \cdot \begin{pmatrix} -U^{(0,2,0)}(\mathbf{r}) - U^{(0,0,2)}(\mathbf{r}) & U^{(1,1,0)}(\mathbf{r}) & U^{(1,0,1)}(\mathbf{r}) \\ U^{(1,1,0)}(\mathbf{r}) & -U^{(2,0,0)}(\mathbf{r}) - U^{(0,0,2)}(\mathbf{r}) & U^{(0,1,1)}(\mathbf{r}) \\ U^{(1,0,1)}(\mathbf{r}) & U^{(0,1,1)}(\mathbf{r}) & -U^{(2,0,0)}(\mathbf{r}) - U^{(0,2,0)}(\mathbf{r}) \end{pmatrix},$$

and the explicit formulas for the potentials are:

$$U^{(1,1,0)}(\mathbf{r}) = \sum_{i,j,k,\alpha,\beta,\gamma=\pm 1} i\,j\,k\,\alpha\,\beta\,\gamma\,F_2\big(z + (k+\gamma)\tfrac{c}{2}, x + (i+\alpha)\tfrac{a}{2}, y + (j+\beta)\tfrac{b}{2}\big),$$

$$U^{(0,1,1)}(\mathbf{r}) = \sum_{i,j,k,\alpha,\beta,\gamma=\pm 1} i\,j\,k\,\alpha\,\beta\,\gamma\,F_2\big(x + (i+\alpha)\tfrac{a}{2}, y + (j+\beta)\tfrac{b}{2}, z + (k+\gamma)\tfrac{c}{2}\big),$$

$$U^{(1,0,1)}(\mathbf{r}) = \sum_{i,j,k,\alpha,\beta,\gamma=\pm 1} i\,j\,k\,\alpha\,\beta\,\gamma\,F_2\big(y + (j+\beta)\tfrac{b}{2}, z + (k+\gamma)\tfrac{c}{2}, x + (i+\alpha)\tfrac{a}{2}\big),$$

$$U^{(2,0,0)}(\mathbf{r}) = \sum_{i,j,k,\alpha,\beta,\gamma=\pm 1} i\,j\,k\,\alpha\,\beta\,\gamma\,F_3\big(x + (i+\alpha)\tfrac{a}{2}, y + (j+\beta)\tfrac{b}{2}, z + (k+\gamma)\tfrac{c}{2}\big),$$

$$U^{(0,2,0)}(\mathbf{r}) = \sum_{i,j,k,\alpha,\beta,\gamma=\pm 1} i\,j\,k\,\alpha\,\beta\,\gamma\,F_3\big(y + (j+\beta)\tfrac{b}{2}, z + (k+\gamma)\tfrac{c}{2}, x + (i+\alpha)\tfrac{a}{2}\big),$$

$$U^{(0,0,2)}(\mathbf{r}) = \sum_{i,j,k,\alpha,\beta,\gamma=\pm 1} i\,j\,k\,\alpha\,\beta\,\gamma\,F_3\big(z + (k+\gamma)\tfrac{c}{2}, x + (i+\alpha)\tfrac{a}{2}, y + (j+\beta)\tfrac{b}{2}\big),$$

where we use two additional auxiliary functions:

$$F_2(u,v,w) = -\frac{vwR}{3} - \frac{u^3}{6}\arctan\left(\frac{v\,w}{u\,R}\right) - \frac{u\,v^2}{2}\arctan\left(\frac{u\,w}{v\,R}\right) - \frac{u\,w^2}{2}\arctan\left(\frac{u\,v}{w\,R}\right) +$$

$$+ u\,v\,w\,\mathrm{artanh}\left(\frac{u}{R}\right) + \frac{3\,u^2\,w - w^3}{6}\mathrm{artanh}\left(\frac{v}{R}\right) + \frac{3\,u^2\,v - v^3}{6}\mathrm{artanh}\left(\frac{w}{R}\right),$$

and

$$F_3(u,v,w) = \frac{3u^2 - R^2}{6}R - u\,v\,w\,\arctan\left(\frac{v\,w}{u\,R}\right) +$$

$$+ \frac{v\,(w^2 - u^2)}{2}\mathrm{artanh}\left(\frac{v}{R}\right) + \frac{w\,(v^2 - u^2)}{2}\mathrm{artanh}\left(\frac{w}{R}\right).$$

Let us denote by $\mathbf{M}_{\mathrm{disp}}$ the magnetization of the displaced cuboid and then the mutual energy (in J) of two cubes:

$$(A6) \qquad W = a\,b\,c\,\mathbf{B}_{\mathrm{avg}} \cdot \mathbf{M}_{\mathrm{disp}}.$$

The interaction of a cuboid with itself is characterized by demagnetizing factors:

$$
D_x = 1 + \frac{U^{(0,2,0)}(0) + U^{(0,0,2)}(0)}{4\pi\,a\,b\,c},
$$

(A7)
$$
D_y = 1 + \frac{U^{(2,0,0)}(0) + U^{(0,0,2)}(0)}{4\pi\,a\,b\,c},
$$

$$
D_z = 1 + \frac{U^{(2,0,0)}(0) + U^{(0,2,0)}(0)}{4\pi\,a\,b\,c}.
$$

Formulas (A7) involve the use of only the auxiliary function F_3 and are therefore somewhat simpler than the long formula suggested by Aharoni [2]. In the special case when a cuboid is a cube, i.e., if $a = b = c$, we obtain the same factors as for the sphere [55]: $D_x = D_y = D_z = \frac{1}{3}$.

APPENDIX B. INTEGRAL REPRESENTATION OF SUMMAND FUNCTION FOR CUBOIDS

In the case of cuboids as defined in Theorem 2.3, the double integral for the single summand can be evaluated semi-analytically as follows. The result serves as an alternative to formulas derived in A for $\nu = 1$ and follows directly from the integral representation of the Crandall functions. The single summand for the cuboid $\Omega = \prod_{\ell=1}^{d}[-c_\ell/2, c_\ell/2]$ in Theorem 2.3 admits the representation

$$
S^{(\boldsymbol{m})}(\boldsymbol{r}) = 2c_1^2 c_2^2 \ldots c_d^2 \int_0^\infty t^{-\nu} \prod_{\ell=1}^{d} \psi_{\alpha_\ell}(r_\ell, t, c_\ell)\frac{\mathrm{d}t}{t},
$$

where the integral can be mermorphically continued to $\nu \in \mathbb{C}$ by means of the Hadamard integral [37, 19]. The functions ψ_m read

$$
\psi_m(r, t, c) = \frac{1}{c^2}\int_{-c/2}^{c/2} \partial_{r'}^m \int_{-c/2}^{c/2} e^{-\pi(r+r'-r'')/t^2}\,\mathrm{d}r''\,\mathrm{d}r', \quad m \in \{0, 1, 2\}.
$$

and the double integral can be evaluated as follows

$$
\psi_m(r, t, c) = t^{-m}(t/c)^2\Big(f^{(m)}\big((r-c)/t\big) - 2f^{(m)}(r/t) + f^{(m)}\big((r+c)/t\big),
$$

with the function f defined as

$$
f(r) = e^{-\pi r^2}/(2\pi) + r\,\mathrm{erf}(\sqrt{\pi}r)/2,
$$

and its derivatives

$$
f'(r) = \mathrm{erf}(\sqrt{\pi}r)/2, \quad f''(r) = e^{-\pi r^2},
$$

with erf denoting the error function.

Appendix C. Glossary of symbols and terms

Table 4. Table of symbols and terms.

Symbol	Meaning
$\subset$	subset of, used for finite or compact subsets
$\subseteq$	subset of or equal to, used for possibly unbounded sets
$\setminus$	set-theoretic difference
$\{a\}$	set consisting of a single element a
!	factorial
sup	supremum
dist	distance
diam	diameter
Vol	volume
$\|\boldsymbol{r}\|_\infty$	infinity norm = maximum absolute element
$\mathbb{R}^d$	d-dimensional Euclidean space
$\mathbb{R}_+$	positive real numbers
$\mathbb{N}$	natural numbers including zero
$\mathbb{N}^n$	n-tuple of numbers from $\mathbb{N}$
$\mathbb{N}_+$	positive natural numbers
$\mathbb{Z}$	integers
$\mathbb{Z}^d$	d-tuple of numbers from $\mathbb{Z}$
$\mathbb{C}$	complex numbers
∇	gradient
Λ	n-dimensional Bravais lattice

References

[1] Claas Abert et al. "magnum.fe: A micromagnetic finite-element simulation code based on FEniCS". In: *Journal of Magnetism and Magnetic Materials* 345 (2013), pp. 29–35. ISSN: 0304-8853. DOI: https://doi.org/10.1016/j.jmmm.2013.05.051. URL: https://www.sciencedirect.com/science/article/pii/S0304885313004022.

[2] Amikam Aharoni. "Demagnetizing factors for rectangular ferromagnetic prisms". In: *Journal of Applied Physics* 83.6 (Mar. 1998), pp. 3432–3434. ISSN: 0021-8979. DOI: 10.1063/1.367113. URL: https://doi.org/10.1063/1.367113.

[3] Amikam Aharoni. "Some Recent Developments in Micromagnetics at the Weizmann Institute of Science". In: *Journal of Applied Physics* 30.4 (1959), S70–S78. DOI: 10.1063/1.2185971. eprint: https://doi.org/10.1063/1.2185971. URL: https://doi.org/10.1063/1.2185971.

[4] A. Arrott and J. E. Goldman. "Fundamentals of Ferromagnetism". In: *Electrical Manufacturing* 63 (3 Mar. 1959), pp. 109–140. URL: https://archive.org/details/sim_electro-technology-newsletter_1959-03_63_3.

[5] P. Asselin and A. Thiele. "On the field Lagrangians in micromagnetics". In: *IEEE Transactions on Magnetics* 22.6 (1986), pp. 1876–1880. DOI: 10.1109/TMAG.1986.1064664. URL: https://doi.org/10.1109/TMAG.1986.1064664.

[6] M. Bebendorf. "Approximation of Boundary Element Matrices". In: *Numer. Math.* 86 (2000), pp. 565–589.

[7]   M. Bebendorf and S. Rjasanow. "Adaptive Low-Rank Approximation of Collocation Matrices". In: *Computing* 70 (2003), pp. 1–24.

[8]   Anne Bernand-Mantel, Valeriy V. Slastikov, and Cyrill B. Muratov. "Asymptotically exact formulas for the stripe domain period in ultrathin ferromagnetic films with out-of-plane anisotropy". In: *Phys. Rev. B* 111 (18 May 2025), p. 184423. DOI: 10.1103/PhysRevB.111.184423. URL: https://link.aps.org/doi/10.1103/PhysRevB.111.184423.

[9]   S. Börm. *Efficient Numerical Methods for Non-local Operators*. European Mathematical Society, 2010.

[10]   J. Borwein et al. *Lattice Sums Then and Now*. Encyclopedia of Mathematics and its Applications. Cambridge University Press, 2013. URL: https://doi.org/10.1017/CBO9781139626804.

[11]   Jonathan M. Borwein and Peter B. Borwein. *Pi and the AGM: a study in the analytic number theory and computational complexity*. Wiley-Interscience, United States, 1987.

[12]   W. F. Brown. *Magnetostatic Principles in Ferromagnetism*. Selected Topics in Solid State Physics, Vol. 1. North-Holland, Amsterdam, 1962.

[13]   W. F. Brown. *Micromagnetics*. Interscience Tracts on Physics and Astronomy, Vol. 18. Interscience Publishers, Wiley & Sons, 1963.

[14]   William Fuller Brown. "Micromagnetics: Successor to domain theory?" In: *J. Phys. Radium* 20 (1959), pp. 101–104. DOI: 10.1051/jphysrad:01959002002-3010100. URL: https://doi.org/10.1051/jphysrad:01959002002-3010100.

[15]   Florian Bruckner et al. "magnum.np: a PyTorch based GPU enhanced finite difference micromagnetic simulation framework for high level development and inverse design". In: *Scientific Reports* 13.1 (July 2023), p. 12054. ISSN: 2045-2322. DOI: 10.1038/s41598-023-39192-5. URL: https://doi.org/10.1038/s41598-023-39192-5.

[16]   Andreas Buchheit, Torsten Keßler, and Kirill Serkh. "On the computation of lattice sums without translational invariance". In: *Mathematics of Computation* 94.355 (2025), pp. 2533–2574. URL: https://doi.org/10.1090/mcom/4024.

[17]   Andreas A Buchheit, Jonathan Busse, and Ruben Gutendorf. "Computation and properties of the Epstein zeta function with high-performance implementation in EpsteinLib". In: *arXiv preprint arXiv:2412.16317* (2024).

[18]   Andreas A Buchheit and Torsten Keßler. "On the Efficient Computation of Large Scale Singular Sums with Applications to Long-Range Forces in Crystal Lattices". In: *J. Sci. Comput.* 90.1 (2022), pp. 1–20. DOI: 10.1007/s10915-021-01731-5. URL: https://doi.org/10.1007/s10915-021-01731-5.

[19]   Andreas A Buchheit et al. "Exact continuum representation of long-range interacting systems and emerging exotic phases in unconventional superconductors". In: *Physical Review Research* 5.4 (2023), p. 043065. DOI: https://doi.org/10.1103/PhysRevResearch.5.043065.

[20]   Andreas A. Buchheit, Jonathan Busse, and Ruben Gutendorf. *Computation and Properties of the Epstein Zeta Function with High-Performance Implementation in EpsteinLib*. Dec. 2024. DOI: 10.48550/arXiv.2412.16317. arXiv: 2412.16317 [math]. (Visited on 03/13/2025).

[21] Andreas A. Buchheit and Jonathan K. Busse. *Epstein Zeta Method for Many-Body Lattice Sums*. 2025. DOI: 10.48550/ARXIV.2504.11989. (Visited on 04/28/2025).

[22] H. Cheng, L. Greengard, and V. Rokhlin. "A Fast Adaptive Multipole Algorithm in Three Dimensions". In: *J. Comput. Phys.* 155 (1999), pp. 468–498.

[23] D. J. Craik and R. S. Tebble. *Ferromagnetism and Ferromagnetic Domains*. Selected Topics in Solid State Physics, Vol. 4. North-Holland, Amsterdam, 1965.

[24] R. Crandall. "Unified algorithms for polylogarithm, L-series, and zeta variants". In: *Algorithmic Reflections: Selected Works*. PSIpress, 2012.

[25] Antonio DeSimone et al. "Recent Analytical Developments in Micromagnetics". In: *The Science of Hysteresis*. Ed. by Giorgio Bertotti and Isaak D. Mayergoyz. Oxford: Academic Press, 2006, pp. 269–381. ISBN: 978-0-12-480874-4. DOI: 10.1016/B978-012480874-4/50015-4. URL: https://www.sciencedirect.com/science/article/pii/B9780124808744500154.

[26] Giovanni Di Fratta et al. "Variational Principles of Micromagnetics Revisited". In: *SIAM Journal on Mathematical Analysis* 52.4 (2020), pp. 3580–3599. DOI: 10.1137/19M1261365. URL: https://doi.org/10.1137/19M1261365.

[27] M. J. Donahue and D. Porter. *OOMMF Software*. http://math.nist.gov/oommf/.

[28] Vladimir Druskin, Stefan Güttel, and Leonid Knizhnerman. "Near-Optimal Perfectly Matched Layers for Indefinite Helmholtz Problems". In: *SIAM Review* 58.1 (2016), pp. 90–116. DOI: 10.1137/140966927. URL: https://doi.org/10.1137/140966927.

[29] P. Epstein. "Zur Theorie allgemeiner Zetafunctionen". In: *Math. Ann.* 56 (1903), pp. 615–644. URL: https://doi.org/10.1007/BF01444309.

[30] P. Epstein. "Zur Theorie allgemeiner Zetafunktionen. II". In: *Math. Ann.* 63 (1906), pp. 205–216. URL: https://doi.org/10.1007/BF01449900.

[31] A. Erdeley, ed. *Higher Transcendental Functions, Volume 2*. McGraw-Hill, 1953.

[32] Olle Eriksson et al. *Atomistic Spin Dynamics: Foundations and Applications*. Oxford University Press, Feb. 2017. ISBN: 9780198788669. DOI: 10.1093/oso/9780198788669.001.0001. URL: https://doi.org/10.1093/oso/9780198788669.001.0001.

[33] E. A. Essex. "Hertz vector potentials of electromagnetic theory". In: *American Journal of Physics* 45.11 (Nov. 1977), pp. 1099–1101. ISSN: 0002-9505. DOI: 10.1119/1.10955. URL: https://doi.org/10.1119/1.10955.

[34] P. P. Ewald. "Die Berechnung optischer und elektrostatischer Gitterpotentiale". In: *Ann. d. Physik* 369 (3 1921), pp. 253–287. DOI: 10.1002/andp.19213690304.

[35] Lukas Exl et al. "Preconditioned nonlinear conjugate gradient method for micromagnetic energy minimization". In: *Computer Physics Communications* 235 (2019), pp. 179–186. ISSN: 0010-4655. DOI: https://doi.org/10.1016/j.cpc.2018.09.004. URL: https://www.sciencedirect.com/science/article/pii/S0010465518303187.

[36]   Hans Fangohr et al. "Vision for unified micromagnetic modeling (UMM) with Ubermag". In: *AIP Advances* 14.1 (Jan. 2024), p. 015138. ISSN: 2158-3226. DOI: `10.1063/9.0000661`. URL: `https://doi.org/10.1063/9.0000661`.

[37]   I. M. Gel'fand and G. E. Shilov. *Generalized Functions. Volume I. Properties and Operations*. Academic Press, 1964.

[38]   Nicolas Giovambattista, Peter J. Rossky, and Pablo G. Debenedetti. "Phase Transitions Induced by Nanoconfinement in Liquid Water". In: *Phys. Rev. Lett.* 102 (5 Feb. 2009), p. 050603. DOI: `10.1103/PhysRevLett.102.050603`. URL: `https://link.aps.org/doi/10.1103/PhysRevLett.102.050603`.

[39]   P. Goetgheluck. "Computing Binomial Coefficients". In: *The American Mathematical Monthly* 94.4 (Apr. 1987), pp. 360–365. ISSN: 0002-9890, 1930-0972. DOI: `10.1080/00029890.1987.12000648`. (Visited on 05/12/2025).

[40]   L. Greengard and V. Rokhlin. "A new version of the Fast Multipole Method for the Laplace equation in three dimensions". In: *Acta Numer.* 6 (1997), pp. 229–269.

[41]   Frank E. Harris. "Incomplete Bessel, Generalized Incomplete Gamma, or Leaky Aquifer Functions". In: *Journal of Computational and Applied Mathematics* 215.1 (May 2008), pp. 260–269. ISSN: 03770427. DOI: `10.1016/j.cam.2007.04.008`. (Visited on 05/09/2025).

[42]   Riccardo Hertel. "Guided Spin Waves". In: *Handbook of Magnetism and Advanced Magnetic Materials*. John Wiley & Sons, Ltd, 2007. ISBN: 9780470022184. DOI: `https://doi.org/10.1002/9780470022184.hmm212`. URL: `https://onlinelibrary.wiley.com/doi/abs/10.1002/9780470022184.hmm212`.

[43]   Alex Hubert and Rudolf Schäfer. *Magnetic Domains: The Analysis of Magnetic Microstructures*. Springer, Berlin, Heidelberg, 1998. DOI: `10.1007/978-3-540-85054-0`. URL: `https://doi.org/10.1007/978-3-540-85054-0`.

[44]   David Ingerman, Vladimir Druskin, and Leonid Knizhnerman. "Optimal finite difference grids and rational approximations of the square root I. Elliptic problems". In: *Communications on Pure and Applied Mathematics* 53.8 (2000), pp. 1039–1066. DOI: `10.1002/1097-0312(200008)53:8<1039::AID-CPA4>3.0.CO;2-I`. URL: `https://doi.org/10.1002/1097-0312(200008)53:8%3C1039::AID-CPA4%3E3.0.CO;2-I`.

[45]   Elizabeth M. Jefremovas et al. "The role of magnetic dipolar interactions in skyrmion lattices". In: *Newton* 1.2 (2025), p. 100036. ISSN: 2950-6360. DOI: `https://doi.org/10.1016/j.newton.2025.100036`. URL: `https://www.sciencedirect.com/science/article/pii/S2950636025000283`.

[46]   C. Kittel and J. K. Galt. "Ferromagnetic Domain Theory". In: ed. by Frederick Seitz and David Turnbull. Vol. 3. Solid State Physics. Academic Press, 1956, pp. 437–564. DOI: `https://doi.org/10.1016/S0081-1947(08)60136-8`. URL: `https://www.sciencedirect.com/science/article/pii/S0081194708601368`.

[47]   L. D. Landau and E. M. Lifshitz. "Theory of the dispersion of magnetic permeability in ferromagnetic bodies". In: *Phys. Z. Sowietunion* 8 (1935), pp. 153–169.

[48]   K M Lebecki, M J Donahue, and M W Gutowski. "Periodic boundary conditions for demagnetization interactions in micromagnetic simulations". In: *Journal of Physics D: Applied Physics* 41.17 (Aug. 2008), p. 175005. DOI:

10.1088/0022-3727/41/17/175005. URL: https://dx.doi.org/10.1088/0022-3727/41/17/175005.

[49] Serban Lepadatu. "Boris computational spintronics—High performance multi-mesh magnetic and spin transport modeling software". In: *Journal of Applied Physics* 128.24 (Dec. 2020), p. 243902. ISSN: 0021-8979. DOI: 10.1063/5.0024382. eprint: https://pubs.aip.org/aip/jap/article-pdf/doi/10.1063/5.0024382/15257104/243902_1_online.pdf. URL: https://doi.org/10.1063/5.0024382.

[50] Igor A. Lukyanchuk et al. "Topological foundations of ferroelectricity". In: *Physics Reports* 1110 (2025). Topological foundations of ferroelectricity, pp. 1–56. ISSN: 0370-1573. DOI: https://doi.org/10.1016/j.physrep.2025.01.002. URL: https://www.sciencedirect.com/science/article/pii/S0370157325000225.

[51] W. D. MacMillan. *The theory of the potential*. McGraw-Hill, New York, 1930. URL: https://catalog.hathitrust.org/Record/000584021.

[52] A. P. Malozemoff and J. C. Slonczewski. *Magnetic Domain Walls in Bubble Materials*. Academic Press, New York, 1979. ISBN: 0120029510.

[53] C.B. Muratov and V.V. Osipov. "Optimal grid-based methods for thin film micromagnetics simulations". In: *Journal of Computational Physics* 216.2 (2006), pp. 637–653. ISSN: 0021-9991. DOI: https://doi.org/10.1016/j.jcp.2005.12.018. URL: https://www.sciencedirect.com/science/article/pii/S0021999106000040.

[54] G. F. Nataf et al. "Domain-wall engineering and topological defects in ferroelectric and ferroelastic materials". In: *Nature Reviews Physics* 2.11 (Nov. 2020), pp. 634–648. ISSN: 2522-5820. DOI: 10.1038/s42254-020-0235-z. URL: https://doi.org/10.1038/s42254-020-0235-z.

[55] Andrew J. Newell, Wyn Williams, and David J. Dunlop. "A generalization of the demagnetizing tensor for nonuniform magnetization". In: *Journal of Geophysical Research: Solid Earth* 98.B6 (1993), pp. 9551–9555. DOI: https://doi.org/10.1029/93JB00694. URL: https://agupubs.onlinelibrary.wiley.com/doi/abs/10.1029/93JB00694.

[56] Nobuo Hayashi Nobuo Hayashi, Koji Saito Koji Saito, and Yoshinobu Nakatani Yoshinobu Nakatani. "Calculation of Demagnetizing Field Distribution Based on Fast Fourier Transform of Convolution". In: *Japanese Journal of Applied Physics* 35.12R (Dec. 1996), p. 6065. DOI: 10.1143/JJAP.35.6065. URL: https://dx.doi.org/10.1143/JJAP.35.6065.

[57] L. Pierobon et al. "Collective antiskyrmion-mediated phase transition and defect-induced melting in chiral magnetic films". In: *Scientific Reports* 8.1 (Nov. 2018), p. 16675. ISSN: 2045-2322. DOI: 10.1038/s41598-018-34526-0. URL: https://doi.org/10.1038/s41598-018-34526-0.

[58] P. Rhodes and G. Rowlands. "Demagnetising Energies of Uniformly Magnetised Rectangular Blocks". In: *Proc. Leeds Phil. Liter. Soc* 6 (1954), pp. 191–210.

[59] Andres Robles-Navarro et al. "Exact lattice summations for Lennard-Jones potentials coupled to a three-body Axilrod–Teller–Muto term applied to cuboidal phase transitions". In: *The Journal of Chemical Physics* 163.9 (Sept. 2025), p. 094104. ISSN: 0021-9606. DOI: 10.1063/5.0276677. eprint: https://pubs.aip.org/aip/jcp/article-pdf/doi/10.1063/5.0276677/

20674844/094104_1_5.0276677.pdf. URL: https://doi.org/10.1063/5.
0276677.

[60] M. Schabes and A. Aharoni. "Magnetostatic interaction fields for a three-dimensional array of ferromagnetic cubes". In: *IEEE Transactions on Magnetics* 23.6 (1987), pp. 3882–3888. DOI: 10.1109/TMAG.1987.1065775.

[61] Thomas Schrefl et al. "Numerical Methods in Micromagnetics (Finite Element Method)". In: *Handbook of Magnetism and Advanced Magnetic Materials*. John Wiley & Sons, Ltd, 2007. ISBN: 9780470022184. DOI: https://doi.org/10.1002/9780470022184.hmm203. URL: https://onlinelibrary.wiley.com/doi/abs/10.1002/9780470022184.hmm203.

[62] K. Shibata et al. "Temperature and Magnetic Field Dependence of the Internal and Lattice Structures of Skyrmions by Off-Axis Electron Holography". In: *Phys. Rev. Lett.* 118 (8 Feb. 2017), p. 087202. DOI: 10.1103/PhysRevLett.118.087202. URL: https://link.aps.org/doi/10.1103/PhysRevLett.118.087202.

[63] Richard M. Slevinsky and Hassan Safouhi. "A Recursive Algorithm for an Efficient and Accurate Computation of Incomplete Bessel Functions". In: *Numerical Algorithms* 92.1 (Jan. 2023), pp. 973–983. ISSN: 1017-1398, 1572-9265. DOI: 10.1007/s11075-022-01438-0. (Visited on 05/07/2025).

[64] K. H. Stewart. *Ferromagnetic Domains*. Cambridge University Press, 1954.

[65] Attila Szilva et al. "Quantitative theory of magnetic interactions in solids". In: *Rev. Mod. Phys.* 95 (3 Sept. 2023), p. 035004. DOI: 10.1103/RevModPhys.95.035004. URL: https://link.aps.org/doi/10.1103/RevModPhys.95.035004.

[66] Samuel K. Treves et al. "Investigating skyrmion stability and core polarity reversal in $NdMn_2Ge_2$". In: *Scientific Reports* 15.1 (Jan. 2025), p. 461. ISSN: 2045-2322. DOI: 10.1038/s41598-024-82114-2. URL: https://doi.org/10.1038/s41598-024-82114-2.

[67] Arne Vansteenkiste et al. "The design and verification of MuMax3". In: *AIP Advances* 4.10 (Oct. 2014), p. 107133. ISSN: 2158-3226. DOI: 10.1063/1.4899186.

[68] Jörg Waldvogel. "The Newtonian potential of a homogeneous cube". In: *Zeitschrift für angewandte Mathematik und Physik ZAMP* 27.6 (Nov. 1976), pp. 867–871. ISSN: 1420-9039. DOI: 10.1007/BF01595137. URL: https://doi.org/10.1007/BF01595137.

[69] Lalit Yadav et al. "Observation of unprecedented fractional magnetization plateaus in a new Shastry-Sutherland Ising compound". In: *arXiv preprint arXiv:2405.12405* (2024).

[70] S.W. Yuan and H.N. Bertram. "Fast adaptive algorithms for micromagnetics". In: *IEEE Transactions on Magnetics* 28.5 (1992), pp. 2031–2036. DOI: 10.1109/20.179394.

[71] I.J. Zucker. "The Exact Evaluation of Some New Lattice Sums". In: *Symmetry* 9.12 (2017), p. 314. URL: https://doi.org/10.3390/sym9120314.

Department of Mathematics, Saarland University, 66123 Saarbrücken, Germany

Department of Mathematics, Saarland University, 66123 Saarbrücken, Germany, German Aerospace Center (DLR), 51147 Cologne, Germany

Department of Mechanical Engineering, Eindhoven University of Technology, 5600 MB Eindhoven, Netherlands

Department of Physics and Astronomy, Uppsala University, Box-516, Uppsala SE-751 20, Sweden